High-Throughput Screening of Yeast Display Libraries for the Development of Matrix Metalloproteinase Inhibitors

A thesis submitted by

Christopher Ghadban

In partial fulfillment of the requirements for the degree of

Master of Science

in

Bioengineering

Tufts University

August 2017

Adviser: Professor James Van Deventer

Acknowledgements

My heartfelt thanks go to my parents, who have been a firsthand example of the values of kindness, hard-work, and integrity. Thank you for your continuous support of all that we do; for providing the love, support, and encouragement necessary to reach this stage in my life. No words can express how grateful Patrick, Matthew and I are for all that you do. Thank you.

I would like to say special thanks to my advisor, Professor James Van Deventer, for trusting me with this project, and for your support and encouragement throughout this process. No matter the challenge, you remained optimistic and encouraging, while providing me the opportunity to be creative and responsible. Thank you.

My laboratory colleagues also deserve wholehearted appreciation. Haixing Kehoe and Jessica Stieglitz, who have been with me since the beginning and who have so often helped me rise to the next challenge; Haixing, in addition, created the CDR-H3 Library we used so frequently in our work. Jacob Lissoos, who inspired me with his dedication and earnestness. Laura Quinto who created the single binding clones that enable me to verify results. And to each of our more recent members – Sheikh Mahatabuddin, Catherine Lessard, Gregory Berumen, and Niroshan Anandasivam – who helped me become a better researcher and lab member. Thank you.

Abstract

Matrix metalloproteinases (MMPs) have long been considered promising therapeutic targets to understand and combat cancer development and progression. Given the similarity of their structures and enzymatic functions, but the considerable variation of their pro-tumorigenic or tumorigenic suppressive effects, small molecules have proven unsuccessful as therapeutics, and more specific inhibitors are required. Of the 23-member family of human MMPs, strides have been made in the development of specific inhibitors against MMP-2, MMP-9, and MMP-14 using protein-based affinity reagents, suggesting that the specificity of protein binders will enable improved targeting of these proteinases.

In this work, overall goal is the development of improved strategies for identifying MMP inhibitors. We isolate and examine single chain variable fragment (scFv) binders from synthetic antibody libraries in an attempt to isolate cross-reactive inhibitors against murine and human isoforms of MMP-9 as a proof of concept for the generation of novel yeast display libraries in the support of protein-small molecule hybrid (PSMH) development. We further present a rapid, display inhibitor assay to better examine the location effect of binding on enzymatic activity, to aid characterization and the advancement of binders to become PSMHs. Finally, we demonstrate the challenge of multiplexed magnetic bead sorting, meant to simultaneously isolate specific binders to a multitude of antigens from a single protein display library, to expedite the process of high-throughput screening and affinity reagent enrichment.

Table of Contents

List of Figures

High-Throughput Screening of Yeast Display Libraries for the Development of Matrix Metalloproteinase Inhibitors

Chapter 1: Introduction

1.1. Introduction

1.1.1. Affinity Reagents

Affinity reagents describe antibodies, peptides, nucleic acids, and other small molecules that bind larger target molecules to identify, track, capture, or otherwise influence their activity of the target. Their highly specific binding is of great use in therapeutics, diagnostics, and basic biological research. For several decades, animal immunization-derived monoclonal antibodies (mAbs) have been the primary affinity reagent utilized for these various roles[1]. However, there is a substantial and growing concern about the reproducibility and specificity of animal-derived mAbs[2,3]. The need for higher quality affinity reagents for improved specificity and reproducibility has led to the further research and development of recombinant antibody and antibody-fragment-based reagents, as well as alternative protein- and now nucleic acid-based scaffolds (aptamers). Over the past decade, alternative protein scaffolds and nucleic acid-based scaffolds have received growing attention, but have yet to display the intersection of stability, specificity, and versatility of antibodies and antibody fragments for therapeutic use[1].

1.1.1.1. Antibodies and Antibody Fragments

In their native role as key components of the adaptive immune system, antibodies, also known as immunoglobulins (Ig), are large and complex glycoproteins capable of recognition and binding of targets substances (antigens), with the potential for eliciting a broader immune response. Generally represented

as Y-shaped molecules (Figure 1), antibodies are formed by two heavy and two light chains. The tail of the Y-shape, the constant region (Fc domain), interacts with cells such as macrophages that express Fc receptors. The shorter light chains interact with the N-terminus of the heavy chains to form the two antigen binding fragment (Fab) "arms", which are composed of both variable and constant regions. At the end of the Fab domains are six loops of variable amino acid composition known as complementarity determining regions (CDRs), which are responsible for antigen binding[4].

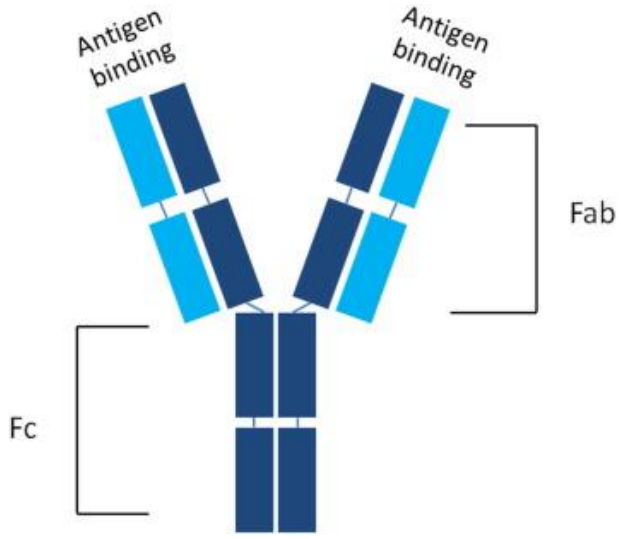

Figure 1. General IgG antibody structure
Displaying the heavy (dark blue) and light (light blue) chains; antigen binding sites; antigen binding fragments (Fab); and constant region (Fc). *Figure adapted from "Modern affinity reagents: Recombinant antibodies and aptamers", Groff et al 2015*[1].

Antibodies remain highly attractive therapeutic agents because of their: (1) high affinity and specificity provided by the CDRs; (2) extended half-lives and well-studied mechanisms of action; and (3) low immunogenicity and toxicity. Various antibody fragment scaffolds that take one or more elements of full-length

antibodies have been created for eased protein expression and application. Indeed, in many cases, the antigen binding fragment (Fab) or a single-chain variable fragment (scFv) is preferable over a full-length IgG to decrease nonspecific binding or interference from other parts of the molecule, or for applications that take advantage of their smaller size[4–6]. scFvs in particular are frequently employed as they are commonly the smallest antibody subunit that can be reliably reproduced and mutated[7]. A single-chain variable fragment (scFv) is not actually an antibody fragment, but instead the fusion of the variable regions of the heavy and light chains of the immunoglobulin, connected with a short linker peptide[8]. These antibody subunits were originally created to facilitate display of the antigen-binding domain as a single peptide on the surface of phage, yeast, and other surface display libraries (see Section 1.3: Protein Libraries)[1,4].

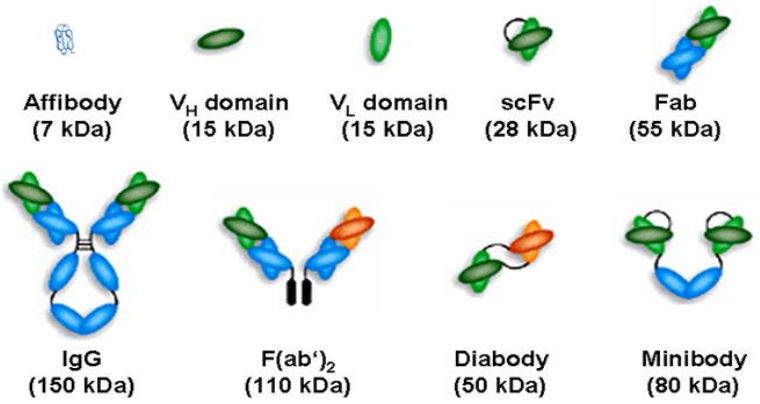

Figure 2. Commonly explored antibody and antibody fragment scaffold depictions

Constant regions are represented in blue; the variable light chains in light green; variable heavy chains by dark green; and the bi-specific heavy and light chains are of dual-binding fragments represented by dark and light orange[80]. *Figure adapted from "Molecular imaging of human epidermal growth factor receptor 2 (HER-2) expression.", Niu et al 2008*[80].

1.1.1.2. Antibody-Drug Conjugates & Protein-Small Molecular Hybrids

The use of antibodies in cancer treatment was first proposed more than a century ago by Paul Ehrlich, the founder of chemotherapy[9]. Early attempts at treatment utilized non-human monoclonal antibodies modified to target human antigens, and therefore evoked a strong immune response against the antibodies themselves. The larger size of the mAbs was also problematic, as it resulted in reduced tumor penetration and so diminished therapeutic effect[10]. Due to these challenges, it was only in 1997 that the United States Food and Drug Administration (US FDA) approved the first anti-cancer antibody, the chimeric mAb rituximab, for the treatment of B-cell non-Hodgkin's lymphoma[11]. Since that time, multiple advances[6,12] in antibody engineering have resulting in a significant increase in the development of antibody-based therapies against cancer[13,14].

Antibodies exhibit a therapeutic effect through one or more of the following mechanisms upon binding: (i) abrogation of tumor cell signaling, resulting in apoptosis; (ii) modulation of T-cell function through antibody-dependent cellular toxicity (ADCC) or complement-dependent cytotoxicity (CDCC); and (iii) exertion of inhibitory effects on tumor vasculature and stroma[15,16]. Despite these mechanisms, most mAbs display insufficient cytotoxicity[17], and current efforts have shifted to focus on combining the selectivity of antibodies and antibody fragments, with the potency of chemotherapeutic small molecules, creating a new class of anti-cancer drugs known as antibody-drug conjugates (ADCs)[18].

ADCs consist of a tumor-specific mAb conjugated to a potent cytotoxin via a stable linker (Figure 3)[19]. Early ADCs offered little improvement over mAbs due

to a lack of internalization of the cytotoxin[20], but with the development of tumor cell internalizing conjugates, their therapeutic potential has increased[21]. Despite these advances, however, it has proven difficult to generate a combined therapeutic agent, with only three ADCs approved and two currently on the market[22], though over 30 are being developed[23].

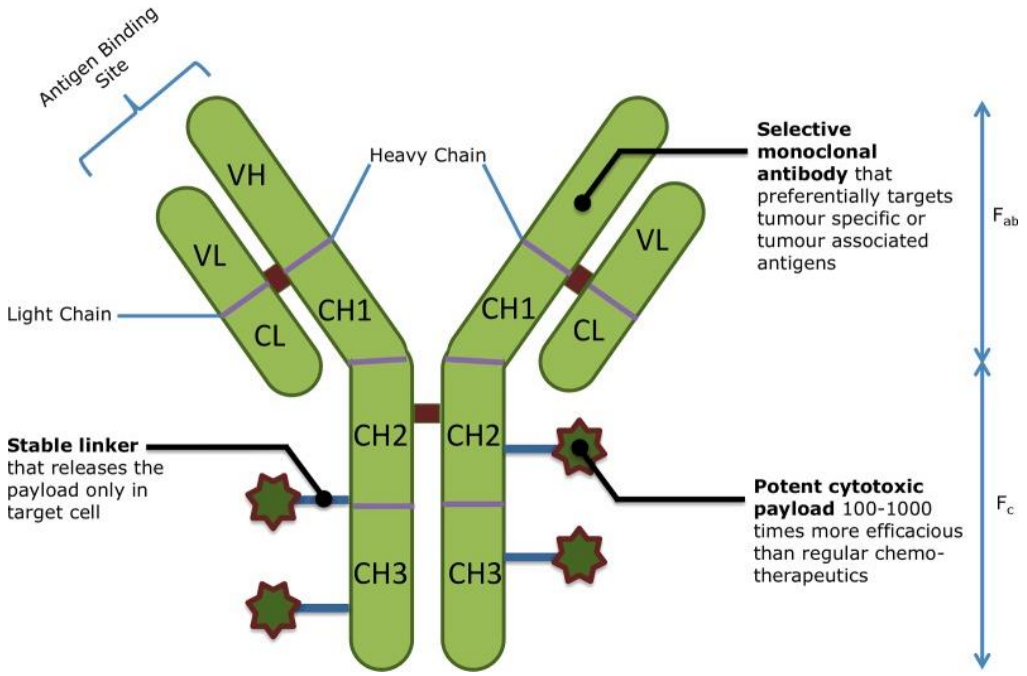

Figure 3. Antibody Drug Conjugate (ADC) Template

Antibody-drug conjugates utilize the selectivity of antibodies combined with stable linkers for targeted release and delivery of potent cytotoxic payloads. *Figure adapted from "Antibody-drug conjugates as novel anti-cancer chemotherapeutics", Peters and Brown, 2015*[21]

Similar in concept, protein-small molecule hybrids (PSMHs, Figure 4) integrate small molecule functionality into binding proteins to create "hybrids" for the discovery of potent, specific inhibitors that cannot be developed using current technologies. These hybrids are distinct from ADCs and related constructs in an

extremely important way: ADCs employ antibody specificity to deliver a small molecular payload to be released once the antibody is bound to the target; PSMHs, however, use chemical functionality to augment molecular recognition of target enzymes and facilitate the disruption of target function. This chemical functionality is introduced by the integration of noncanonical amino acids (ncAAs), and defines unique structures not covered by current classes of therapeutics[24]. The novel approach of combining binding proteins and small molecules will support the discovery of constructs with distinct inhibitory capabilities for direct clinical applications, and use as tool compounds for the elucidation of the effects of single proteins on the tumor microenvironment.

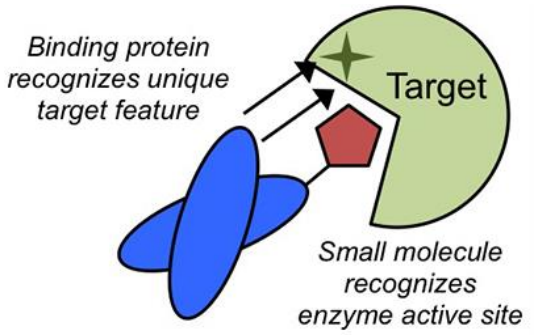

Figure 4. Protein-small molecule hybrid (PSMH) template
Depiction of protein-small molecule hybrid targeting an antigen. The scFv binds to a location near the active site of the specific protein target, delivering the small molecule payload directly to the active site with greater specificity. *Figure adapted from Prof. James Van Deventer.*

1.1.2. Protein Display Libraries

Surface display systems enable the study and screening of proteins and protein-protein interactions on the scale of billions, facilitating important advances in protein engineering, and enabling the generation of compounds and affinity reagents for industrial application, diagnostics, and therapeutic development.

Display platforms have been established around numerous hosts, including: phage[25], gram positive bacteria[26], gram negative bacteria[27], yeast[28], and mammalian cells[29], while additional platforms, such as ribosome display[30], make use of cell free formats. These libraries differ in the proteins they are able to express, technologies that are available for screening, and the size of the library that can be constructed.

With display platforms, combinatorial protein libraries are expressed on the surface of the host and screened using high-throughput techniques to identify mutants of a target phenotype[31]. This genotype-phenotype link is perhaps the most vital component of surface display technologies, as it enables the identification of protein variants isolated through library screens. Properties such as binding affinity, thermal stability, and catalytic efficiency can be measured and isolated against while the proteins remain tethered to the display surface, enabling rapid isolation and characterization of individual mutants[32].

Protein display libraries are typically designed around the sequences of one or more starting proteins with properties similar to those of the required target. Design and construction is based around two, often conflicting, goals: conservation and diversification. The proteins must be sufficiently diverse to ensure unique function, while remaining suitably similar to retain fit for the target[31]. When utilizing antibody and antibody fragment scaffolds for novel libraries – particularly for those without extremely specific protein targets – this balance can be more easily achieved by maximizing diversity within the CDRs, while maintaining structure through consistency within the other domains[33].

There are four standard antibody library types, set by the source of sequences used when generating the library: immune, naïve, synthetic, and semi-synthetic[34,35]. Immune antibody libraries are created by the isolation of sequences from active B cells of an immunized animal (usually a mouse). New immune libraries must be generated for each antigen of interest[35] and each library can consist of more than 10^{10} differing antibody clones[36,37]. Naïve antibody libraries utilize resting B cells from healthy, non-immunized humans and have been reported to contain up to 10^{11} clones[36,38]. Semi-synthetic and synthetic libraries consist of either natural and artificial, or exclusively manmade CDRs, respectively[39]. By incorporating synthetic CDR manipulation, synthetic libraries are not bound by natural CDR limitations.

1.1.2.1. Yeast Display Libraries

Of the display platforms and library types available, yeast display has been rapidly gaining traction as a powerful platform for both affinity maturation and novel affinity reagent isolation since its introduction over 15 years ago. Yeast display is distinguished by two key advantages: (1) eukaryotic expression supporting complex protein expression similar to that of mammalian cells, and (2) multi-copy display on the surface of cells that enables quantitative library analysis and screening based on properties including binding affinity, protein stability, and chemical reactions without subcloning, expression, or purification of the displayed protein[40]. In addition, yeast display libraries are faster growing, more robust, and able to reach a greater clonal diversity than mammalian display libraries[41,42].

Yeast display platforms primarily employ cell wall anchoring of scFvs via the *Saccharomyces cerevisiae* Aga2 protein linked to a-agglutinin yeast adhesion receptor Aga1 through two disulfide bridges, forming a covalent complex on the surface of the yeast cell[42] (Figure 6). The Aga1 gene is stably integrated into the yeast chromosome, while the Aga2 gene is encoded within a circular yeast display plasmid vector; both are tightly controlled by galactose-inducible promoter *GAL1*, while the tryptophan producing gene *TRP1* is used for plasmid maintenance in *S.cerevisiae*. For selection and replication in *Escherichia coli*, ampicillin resistance is conferred and a pUC origin added. The yeast display vector employed for the libraries associated with this thesis is pCTCON-2 (Figure 5)[43].

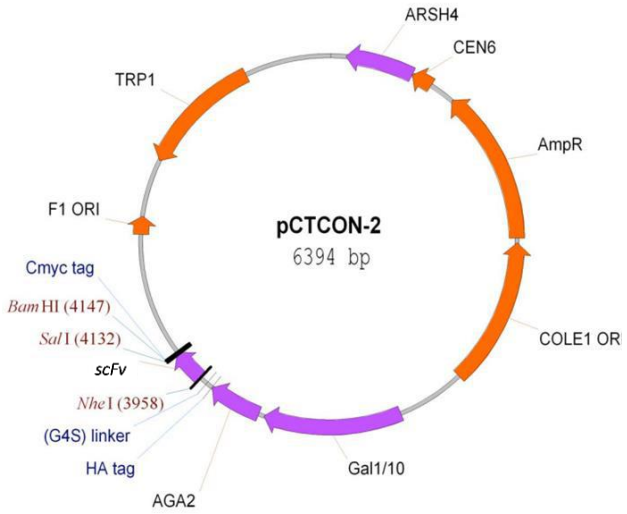

Figure 5. pCTCON-2 vector

This display expression vector incorporates a tightly regulated galactose promoter to trigger production of a scFv with HA and c-Myc epitope tags, while also incorporating ampicillin resistance for selection in *E.coli* and a *TRP1* producing gene for selection in Trp-producing deficient yeast.

When a scFv is integrated for expression, each yeast cell typically displays 1×10^4 to 1×10^5 copies of the protein[43]. Display of the scFv can be measured through flanking hemagglutinin (HA) and c-Myc epitope tags, to ensure full-

expression expression and to assist in detection of target antigen binding for binder isolation and population characterization (Figure 6)[43]. Further, yeast selections and characterizations are performed in solution, allowing precise control of the antigen concentration to establish affinity thresholds, facilitating clone characterization[40].

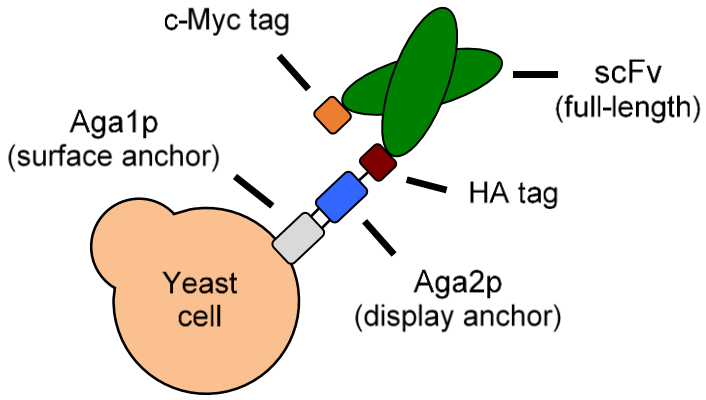

Figure 6. Yeast Display
Schematic of a displayed scFv with binding anchor proteins and display epitope tags on the yeast cell surface using the pCT-CON2 vector.

1.1.2.2. CDR-H3 Library

The CDR-H3 Library is a yeast displayed synthetic scFv library with diversity in the third heavy chain complementarity-determining region (CDR-H3). As has been recently discovered, libraries with diversity focused within the CDR-H3 region are more than sufficient to derive highly specific, nanomolar affinity binders to multiple protein targets[44,45]. By limiting diversity within one CDR, a library has been generated that allows for the greatest possible flexibility when inserting TAG codons within the scFv to enable noncanonical amino acid incorporation for PSMH construction, while simultaneously ensuring the greatest potential diversity for binding. To diversify CDR-H3, varied loops lengths (7-15) were introduced and randomized, with the randomization designed to mimic natural CDR-H3 antibody sequences[45] (Figure 7).

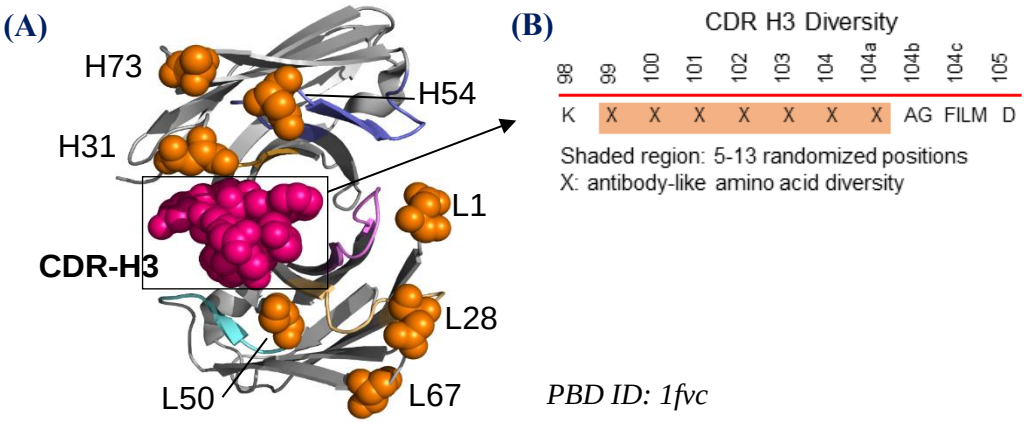

Figure 7. CDR-H3 Library diversity within the CDR-H3 region

(A) The CDR-H3 region is highlighted in pink in the crystal structure of the humanized anti-HER2 antibody. Additionally, potential TAG codon sites are highlighted in orange. **(B)** The diversity of CDR-H3, where the X codon is designed to have amino acid diversity similar to natural antibodies. *Figure adapted from Professor James A. Van Deventer.*

1.1.2.3. Sidhu Library

We also examined the more established synthetic scFv Sidhu Library. While not created for the purpose of generating protease inhibitors, it nevertheless provides a means of potential MMP binder isolation and enables the identification of strategies for isolating inhibitory antibodies. This library was further utilized in the evaluation of multiplex magnetic bead sorting (Chapter 3). The Sidhu Library was constructed based on the phage-displayed scFv library "G"[46], in a manner previously described for synthetic Fab libraries "D" and "F"[47,48]. Diversity was introduced into CDRs L1, L2, H1 and H2 prior to sequence randomization. Two rounds of protein A selections were used to enrich for properly folded and displayed scFvs, and used as a template for introducing diversity into CDRs L3 and H3. Several hundred clones from the phage library were sequenced to validate construction, and the full diversity design is described in Figure 8[46].

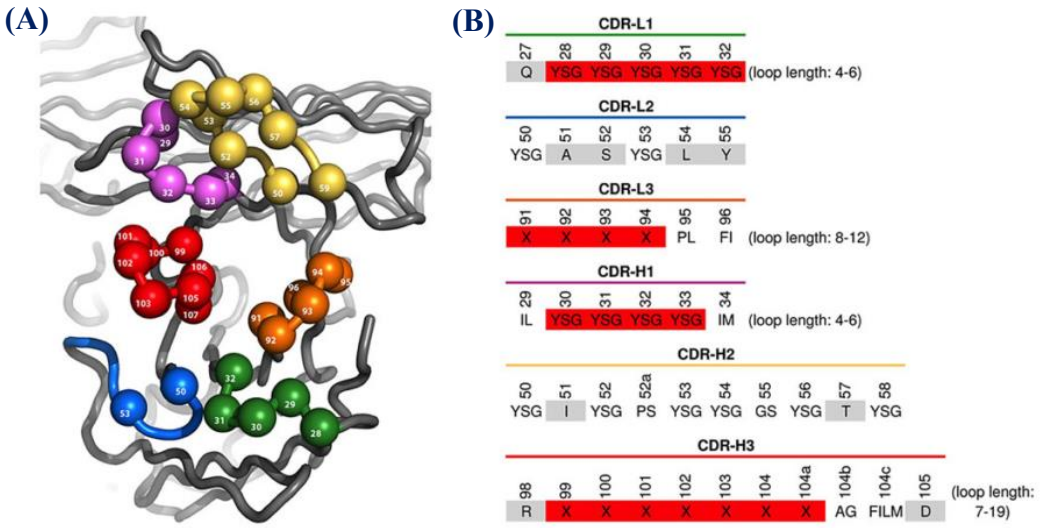

Figure 8. Design of scFv-phage library G, the model for the Sidhu Library

"(A) Structural representation of CDR diversification. Residue numbering is based on the Fab structure 1FVC[49], diversified residues are depicted as spheres. **(B)** CDR diversity design. Segments in red correspond to positions replaced by sections of variable loop length, while grey sections signify non-diversified positions. At diversified positions, allowed amino acids are shown by their single-letter code. "X" represents the following AA mixture: Y (25%), S (20%), G (20%), A (10%), F,W, H, P, V (5% each)." *Figure and caption adapted from "A Switchable Yeast Display/Secretion System", Van Deventer et al., 2015*[46].

1.1.3. High-Throughput Screening with Protein Display Libraries

Protein engineering relies heavily on high-throughput screening for the selective enrichment and isolation of clones with the desired phenotype. Widely used in the biotechnology, pharmaceutical, and institutional research industries, standard high-throughput screening methods include: automated high-throughput screening (AHTS), immobilized antigen sorting (IAS), and flow cytometry. More recently developed techniques such as DNA-barcoded libraries, *in vitro* compartmentalization, and phage-assisted continuous directed evolution (PACE) are also available, but each requires considerable technical expertise[50].

AHTS employs automation to direct the continuous, individual isolation and characterization of potential targets using plate based growth and isolation. This costly method is most frequently utilized by the pharmaceutical industry given the prohibitive cost to most single investigator research laboratories, but enables extensive and thorough library examination. Immobilized antigen sorting is most frequently used for the enrichment and isolation of affinity reagents. IAS exploits the attachment of antigen targets to varied support materials for repeat screening against the library, as a form of biopanning. This technique enables the rapid enrichment of libraries through the removal of clones bound to the antigen attached to the solid target. Of the various forms of IAS, magnetic bead sorting is perhaps the most commonly used and effective. Flow cytometry is also widely used as a powerful platform for quantitative, high-throughput functional analysis of cells and biomolecules using microspheres as solid support. This approach generally operates based on the size and fluorescent labeling of particles passing through an electronic detection apparatus in a single stream[51].

1.1.3.1. Magnetic Bead Sorting

A form of immobilized antigen sorting, magnetic bead sorting (MBS) is perhaps the most commonly employed high-throughput screening technique for initial enrichment of yeast display libraries. MBS enables rapid affinity capture of strong and weak binding interactions among large nonbinding populations for targeted enrichment. The multivalency of the surface selection allows for over

30,000-fold enrichment in a single pass, requiring far less target antigen for each selection than alternative screening techniques[52].

To perform magnetic bead sorting, antigens are attached (through various means) to magnetic particles (of diverse composition and surface chemistry) and then incubated with a display library, a small fraction of which expresses proteins or peptides capable of binding the ligand of interest. Bound cells are removed from the population through incubation against a magnet, while unbound cells are removed and washed away. Cells bound to the magnetic particles can then be cultured (rescue growth) as a population enriched for the target, and the process repeated until a suitable purity of cells displaying target binders is reached[52]. This process is depicted in Figure 9, covered in greater detail in the Experimental Methods of Chapter 2, and explore more in Chapter 3, Multiplexed High-Throughput Screening with Yeast Display.

1.1.3.2. Flow Cytometry and Fluorescence-Activated Cell Sorting (FACS)

Flow cytometry and the related fluorescence-activated cell sorting (FACS), are perhaps the most widely employed of all high-throughput screening methods, unique for their ability to make sensitive, quantitative measurements of molecular interactions in real time[51]. This approach is primarily applied to the detection of fluorescently labeled proteins or ligands bound to specific particle, cell, and tissue samples. By also integrating automated sampling, flow cytometry is a robust and adaptable method for the analysis of molecular interactions.

During flow cytometry, cell suspensions are focused through a small nozzle using sheath fluid to pass single cells through laser light within the cytometer. Light

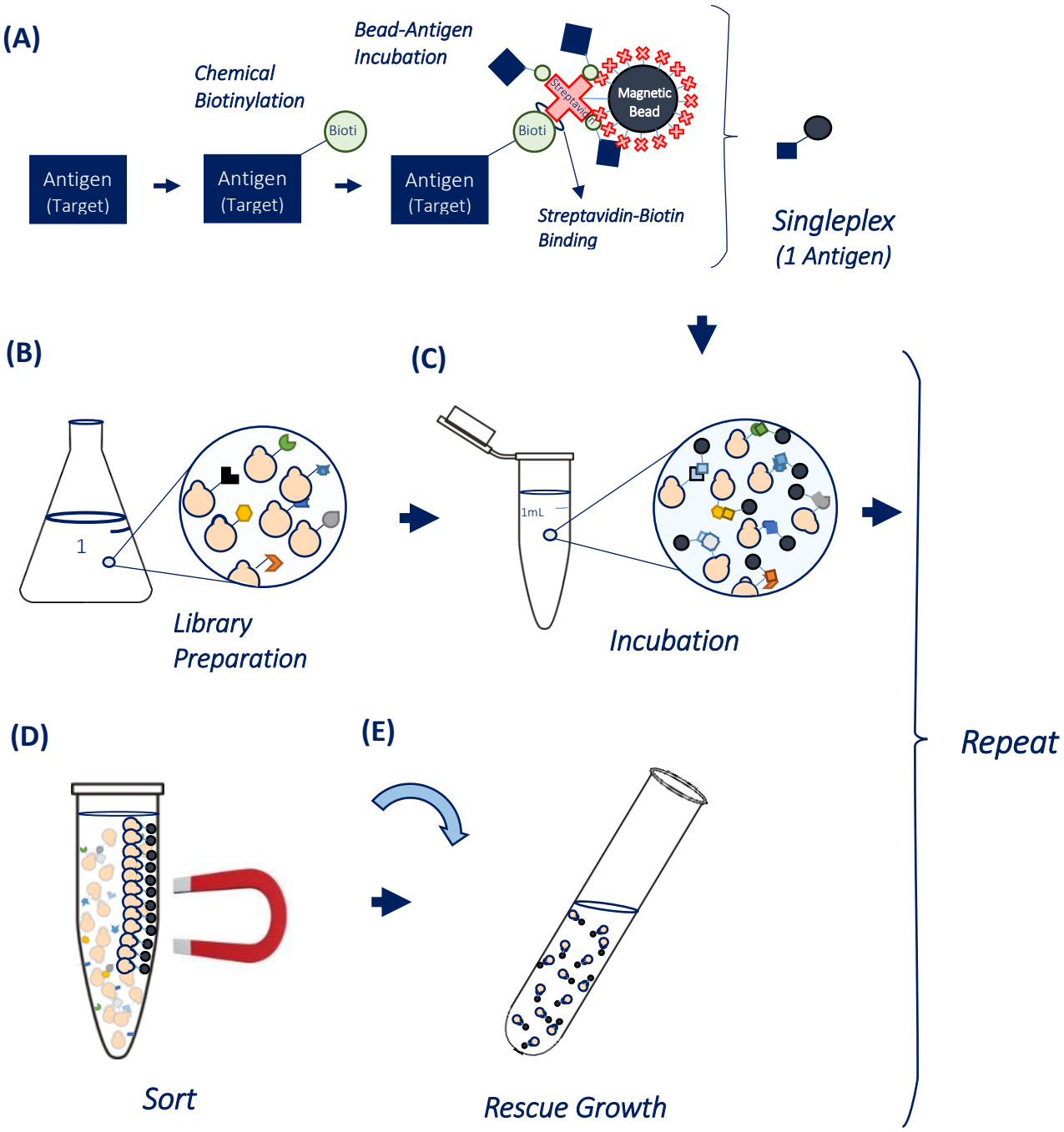

Figure 9. Streptavidin-Biotin Magnetic Bead Sorting

(A) Depiction of the preparation of magnetic beads bound with target antigens via the biotin-streptavidin interaction, one of the strongest non-covalent interactions. Antigens are biotinylated (chemically or enzymatically), and incubated with magnetic beads coated in streptavidin for two hours. **(B)** Simultaneously, a protein display library is prepared by spinning down and washing the cells to ensure removal of excess metabolites before **(C)** a 2 hour incubation of the cells with prepared, antigen-coated magnetic beads. **(D)** Cells bound to the magnetic beads are sorted through removal with a magnetic, and **(E)** rescued to form a population enriched for the antigen target, for either repetition of the MBS or isolation and characterization of select, enriched clones.

is scattered by passing cells or particles, and detected through both forward scatter (FS) and side scatter (SS) detectors, while fluorescence detectors measure positively stained cells or particles. These measurements enable the simultaneous, multi-parameter analysis of single cells, while also providing a template for fluorescence-activated sorting of individual cells[53] (Figure 10).

Fluorescence-activated cell sorting (FACS) utilizes the fluorescent labeling of positive cells and particles to separate those samples which fall within set parameters, as a proxy for direct antigen binding, at a rate of 10^8 cells per hours[52]. FACS allows selection without expression level bias, while also enabling real-time selection based on sample data[52]. When combined with yeast display, it is common to first use forward and side scatter data to ensure selection of single cells, before isolating for those which correspond to fluorescence measurements of both (1) full-length display of the scFv, and (2) the presence of the fluorescently-labeled and bound antigen target.

1.1.3.2.1. Analysis of Flow Cytometry Data

When analyzing flow cytometry data (Figure 11), event plots are first examined in log scale to ensure gating (selection by segmented areas within the graph) of single cells using forward (FSC) and side (SSC) light scattering measurements. Once single cell sample measurements are isolated, fluorescence data may be examined. Frequently, and as performed for this research, dual-color fluorescence labeling is employed to ensure (1) full-length expression of the scFv, and (2) binding of the target antigen. Single color controls enable fluorescence

parameters to be set, while also ensuring that fluorescent reporters do not bind to the yeast surface, so that the appearance of fluorescence dependent on scFv expression and target antigen binding can be assured. By choosing fluorescent labels with minimal or no overlap in their emissions spectra, targeted labeling can be further secured.

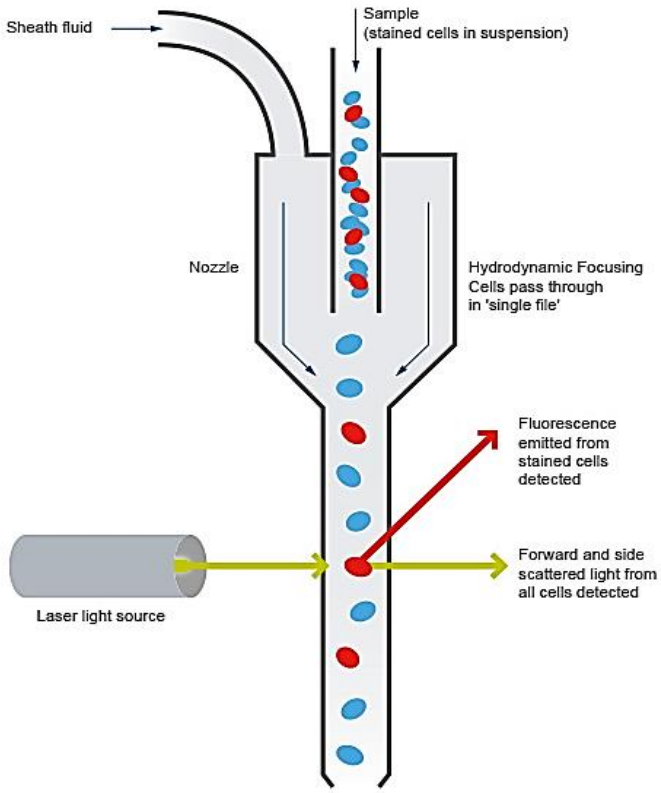

Figure 10. Overview of flow cytometry

Sheath fluid and suspended cells are combined, and hydrodynamic focusing passes individual cells through the nozzle. Laser light is passed through the fluid and sample stream and both forward and side scattered light and fluorescence emissions are collected for further analysis. *Figure adapted from "Introduction to Flow Cytometry", abcam*[53].

In the work to be described in this thesis, labeling for these experiments was such that target antigen binding is expressed by a vertical shift (Q1; Fig. 11 C2) in the cell population, while surface display of the scFv is visualized by a horizontal

shift (Q3; Fig.11 C3). As can be seen in the fluorescent plots of the negative control within Figure 11 C1, Quadrant 4 (Q4) shows the population of cells without surface displayed proteins or bound antigen; in all induced yeast populations, there exists a fraction of cells that remain uninduced. When cells display binders to the target antigen, the population will be shifted both up and to the right, forming a diagonal line in Q2 (Fig.11 B3), the "target population." Those cells which display scFvs but do not bind to the antigen targeted are shifted only to the right (Q3) and make up the "negative, displaying population."

Percent Antigen Binding (Fig.11, B4) is used to compare results from gated fluorescent data, and is calculated by taking the percent of the target displaying population, as compared to the total displaying population:

$$\%\ Antigen\ Binding = \frac{Q2}{Q2+Q3} * 100 \qquad (1.1)$$

$$\frac{Target\ Displaying\ Population}{Total\ Displaying\ Population} * 100 \qquad (1.2)$$

Percent antigen binding is often displayed through bar graphs to more easily visualize enrichment levels between screening rounds, be they magnetic bead sorting or FACS.

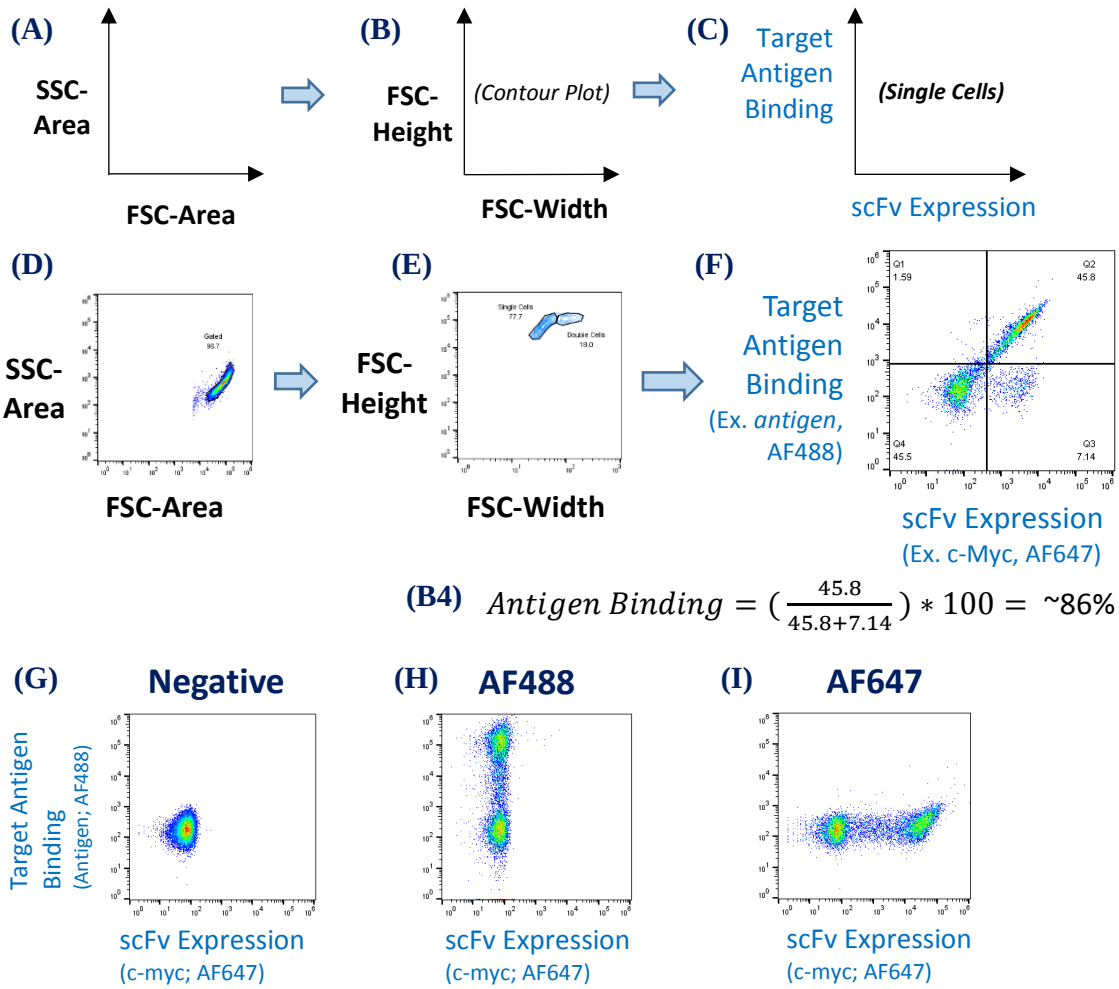

Figure 11. Analysis of Flow Cytometry and FACS Event Plots with Dual-Fluorescent Labeled Yeast Display

The first step to analyzing flow cytometry event plots is to ensure gating for single cells using light scattering measurements. Primary gating **(A, D)** examines forward scattered (FSC) area by side scattered (SSC) area, while secondary gating **(B, E)** utilizes contour plots to select for the single cell population. Once single cells have been selected, fluorescence data may be examined for scFv expression and target antigen binding **(C, F)**. Single color controls **(G, H, I)** are used during the flow cytometry experiment itself, and run directly prior to the samples to ensure (1) proper labeling of the cells, and (2) that visualization of the events falls within the plot area so that settings may be adjusted as needed.

1.1.4. In This Work

The following chapters focus on two projects, which employ high throughput screening of yeast display libraries for the isolation of scFv binders against specific target proteins. Chapter 2 employs both magnetic bead sorting and FACS against the CDR-H3 and Sidhu Libraries to isolate scFvs capable of cross-reactive binding of human and murine MMP-9. It further describes a protocol for the benchtop activation of MMPs, and begins to explore the development of an assay to test and compare protein binding versus inhibition on the yeast cell surface. Chapter 3 explores the Sidhu Library in an attempt to further advance magnetic bead sorting from singleplex (the isolation of binders against a single target antigen), to multiplex (the isolation of multiplex target antigens simultaneously from which the same cell population.

Chapter 2: High-Throughput Matrix Metalloproteinase-9 (MMP-9) Binding Protein Isolation & Yeast Display Inhibitor Assay Development

2.1. Introduction

2.1.1. Overview

Matrix metalloproteinases (MMPs) have long been considered promising therapeutic targets to understand and combat cancer development and progression. Given the similarity of their structure and enzymatic function, but the considerable variation of their pro-tumorigenic or tumorigenic suppressive effects, small molecules have been proven unsuccessful across clinical trials as more specific inhibitors are required. Of the 23-member family of human MMPs, strides have been made in the development of specific inhibitors against MMP-2, MMP-9, and MMP-14 using protein-based affinity reagents. In this work, we examine single chain variable fragment (scFv) binders from synthetic antibody libraries in an attempt to isolate cross-reactive inhibitors against the murine and human isoforms of MMP-9 as a proof of concept for the generation of novel yeast display libraries in the support of protein-small molecule hybrid (PSMH) development. We further present a rapid, display inhibitor assay to better examine the location effect of binding on enzymatic activity, to aid characterization and the advancement of binders to become PSMHs, and demonstrate that cross-reactive isoform binders can be selected by first performing enrichments against single isoforms.

2.1.2. Matrix Metalloproteinases (MMP)

2.1.2.1. MMPs and the Tumor Microenvironment

Traditional cancer research has focused on genetic mutations in cells that result in cancerous phenotypes, but neglected the surrounding tumor microenvironment (TME). Recent work has shown that the TME, in particular the extracellular matrix (ECM), plays a significant role in cancer progression and malignancy outcome[54]. This microenvironment is broadly classified into three main groups: cells of haematopoietic origin, cells of mesenchymal origin, and non-cellular components, the major element of which is the ECM[55]. Of ECM remodeling proteins, matrix metalloproteinases (MMPs) are among the most significant, as their expression levels and functions change dramatically in nearly all human cancers[54]. MMPs are thus tied to tumor aggressiveness, stage, and patient prognosis[56,57] for the multitude of roles they perform within and beyond the TME (Figure 12).

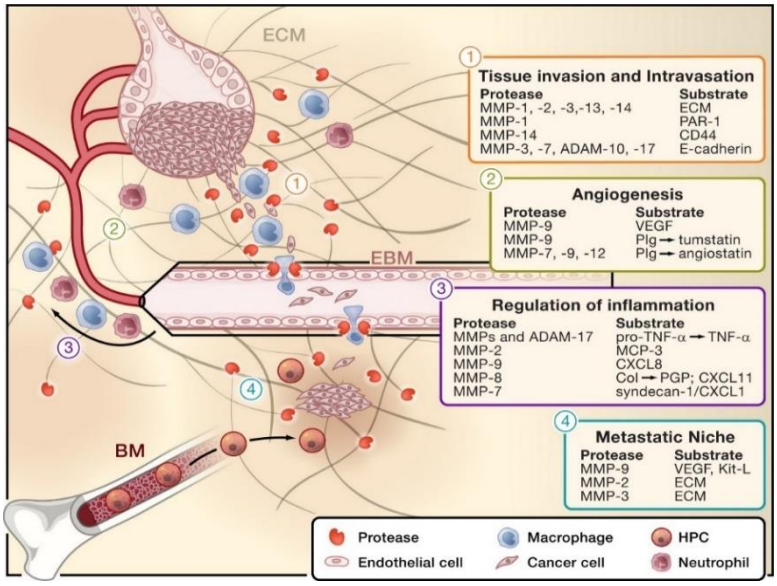

Figure 12. Multiple Functions of MMPs in the Tumor Microenvironment
This figure demonstrates the known roles of several MMPs, highlighting their varied functionality. *Figure adapted from "Matrix metalloproteinases: regulators of the tumor microenvironment", Kessenbrock et al., 2010* [81].

Matrix metalloproteinases (MMPs) are a 23-member family of zinc ion-dependent endopeptidases[58]. All MMPs, except MMP-7 and MMP-26, possess similar structures, containing: a signal peptide, a propeptide domain, a catalytic domain with zinc active site, a hinge region, and a hemopexin domain. MMP-7 and MMP-26 do not contain the hinge region or a hemopexin domain. Most MMPs are expressed in an enzymatically inactive (pro-) state, with a cysteine residue of the pro-domain interacting with the zinc ion of the active site[59] (Figure 2). Through disruption of this interaction (known as cysteine switch) by extracellular proteinases, the enzyme becomes proteolytically active[60].

Matrix metalloproteinases play crucial roles in various physiological processes, including many of the primary activities of cancer cells – autonomous growth, replication, tissue invasion, and metastasis – through intercellular pathway regulation. This regulation is achieved through the degradation of physical barriers, such as the extracellular matrix (ECM)[58]. While many features of MMP proteolytic action are pro-tumorigenic, some MMPs exhibit anti-tumorigenic effects[61,62], and many are involved with normal physiological processes such as reproduction, embryonic development, wound healing, and tissue remodeling[63]. There is an ongoing need to distinguish the specific activities of individual MMPs in order to better understand the effect of individual proteases on the tumor microenvironment and to acquire targets for future therapeutics[64].

2.1.2.2. Current Inhibitor Development Challenges

Matrix metalloproteinases have long been considered promising therapeutic targets for tumor progression, given their regulatory functions on cancer cell physiological activities. However, previous attempts to develop small molecule inhibitors in the form of peptidomimetics (compounds which mimic active site binding targets) failed in clinical trials due to severe side effects resulting from broad blockage of MMPs, including those which were tumorigenesis-suppressing[65]. Therefore, development of selective inhibitors for tumorigenesis-promoting MMPs are highly desired for successful MMP-based therapies. However, the catalytic domains of the 23 MMP family members share high amino acid and structural similarity, and their active sites are extensively conserved. Due to these similarities, researchers have found it an incredible challenge to distinguish between MMPs with small molecule inhibitors[65,66].

Specific MMP inhibition has thus far achieved limited success against MMP-2, MMP-9, and MMP-14 with biological-based inhibitors, including monoclonal antibodies and macromolecular fusion proteins. Small molecular compounds which bind the haemopexin domain and peptides which block dimerized-induced functions have also demonstrated potential[54]. As such, additional protein engineering needs to completed, and isolation methods developed, to expand on these early successes and so generate inhibitors of specific MMP function.

2.1.3. Matrix Metalloproteinase-9 (MMP-9)

Matrix metalloproteinase-9 (MMP-9) is secreted by most human cancer cells, can be secreted by infiltrating immune cells, and contributes to tumor progression, angiogenesis, and tumor cell invasion. Along with MMP-2, MMP-9

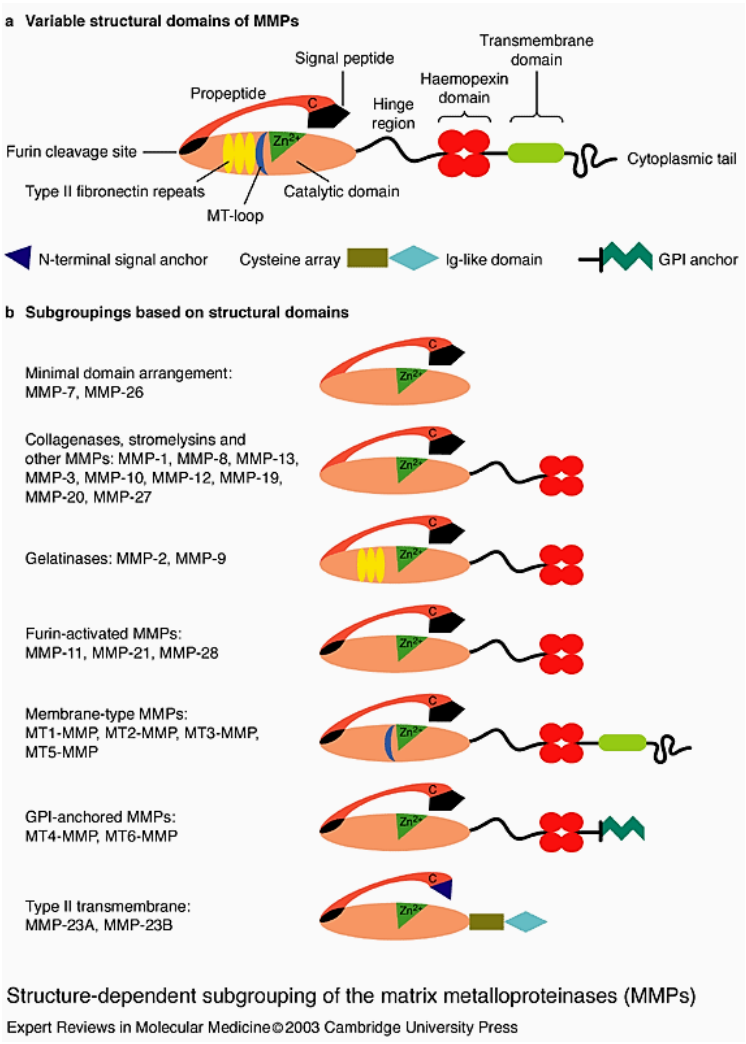

Figure 13. Structure-dependent subgrouping of matrix metalloproteinases
The above depict the structural similarities of MMPs. *Figure adapted from "Metalloproteinases and their inhibitors in angiogenesis", Lafleur et al, 2017*[82].

makes up the gelatinase group within the MMP family. Activation of MMP-9 can be induced in myriad ways, including by inflammatory cytokines, growth factors,

and cell/stroma interactions, particularly in the most malignant cells[54]. By contrast, MMP-2 is thought to be constitutively expressed by many cell types. As such, there is great demand for inhibitors which can differentiate between these extremely similar MMPs.

2.1.4. Time Course MMP-9 Binding for Inhibitor Isolation

When examining proteins enriched against proteinases for inhibitor selection, it is important to ensure that binders isolated are able to withstand cleavage by the enzyme. To this end, extended, time course incubations of the library – enriched or *de novo* – with the active enzyme are essential to ensure sufficient time for enzymatic exposure to the affinity reagent.

By performing these screens prior to enrichment, a library may be more rapidly examined for clonal variants that are able to resist the enzymatic cleavage of the enzyme, and the possibility of isolating an inhibitor against said target against remaining clones will increase. When performing a time course experiment on an enriched library, the possibility of an inhibitor may be lost, but binders may provide a unique opportunity to otherwise inhibit or characterize the enzyme, as well as affording a means of examining the molecular interactions of binding for potentially novel protein engineering of new inhibitors. When combined with protein-small molecule hybrids or antibody-drug conjugates, binders enable a new class of therapeutics for targeted delivery of small molecules for more selective inhibition, while avoiding the more commonly structured active site of enzymes within the same protein family.

2.1.5. MMP-9 Single Clone Binders: M0076-D03 and DX-2802

We work with MMP-9 as a representative matrix metalloproteinase of great therapeutic potential, which has seen some measure of binder and inhibitor success. By comparing binders and inhibitors isolated from the CDR-H3 and Sidhu Libraries with those previously characterized single clones, we are able to validate this methodology of selection, inhibitor assay development, and protein-small molecule hybrid creation. M0076-D03 ("M0076") and DX-2802 are the single clones examined here. These binders were isolated and patented by the Dyax Corporation, prior to their acquisition by Shire Pharmaceuticals, as a potential method of treatment or prevention of systemic sclerosis[67]. Through the work of Van Deventer Laboratory member Laura Quinto, these scFvs were cloned into pCTCON2 (Figure 5) and expressed through the yeast display platform for comparative analysis to isolated binders, and when developing a Yeast Display Inhibitor Assay.

2.1.6. Research Objectives

The overarching goal of this thesis project was the establishment of a process for isolating matrix metalloproteinase binders for PSMH design, through the development of a benchtop means of MMP activation; examination of existing and novel yeast display protein libraries for binder and inhibitor isolation and characterization; and the establishment of a simple display inhibition assay for selecting scFvs capable of serving as the affinity reagents within protein-small molecule hybrids.

2.1.6.1. Isolation (isoform cross-reactivity)

The isolation of cross-reactive binders from yeast display libraries employed magnetic bead sorting to enrich libraries against alternating human and murine isoforms of MMP-9. By enriching for cross-reactive binders, future therapeutic development is more easily accomplished as a majority of pre-clinical studies utilize mouse models. When the libraries are sufficiently enriched, FACS enabled further selection for binders of various categories: weak binders, strong binders, and binders able to resist enzymatic activity. Once populations are sufficiently characterized, individual clones are isolated for sequencing and further, individual, analysis.

2.1.6.2. Characterization

Characterization of individual clones is a time intensive component in any antibody discovery process. While not completed in this work due to time constraints, to characterize isolated affinity reagents each binding clone will need to be sequenced, titrated, and examined with flow cytometry. Sequencing and comparison to existing homological data of known binders and the antigen target may provide insight on protein-protein interactions occurring. Titration experiments provide determinations of dissociation constants (K_D) and off-rates (k_{off}), while isoform cross-reactivity, pro- versus active-form binding, and stability analysis are examined by flow cytometry. Yeast display is perfectly suited for these tasks, as flow cytometry enables direct, quantitative measurements of these binding properties. Grouping of isolated clones into binders and inhibitors is further enabled

by comparison of MMP-9 activity through the Display Inhibition Assay, and all results will be compared to those of pre-existing binders M0076 and DX-2802.

2.2. Results and Discussion

2.2.1. MMP-9 Benchtop Activation

Before sorting against activate MMP-9 could be performed, an activation protocol needed to be established. Using existing protocols[68–70] and knowledge of *in vivo* MMP activations[71,72] as a guide, a simple benchtop activation with trypsin was developed and validated (Figure 14).

With existing activation methods as a base, the following combination was established: MMP (1 mg/mL) + Trypsin (0.5 mg/mL) + Activation Buffer (50 M Tris-HCl, 150 mM NaCl, 5 mM $CaCl_2$), in a ratio of 1:2:7. With the activation completed, the trypsin reaction would be quenched using PMSF (100 mM), adding the same volume as the MMP. The duration and temperature of incubation where then tested using our target, MMP-9. Most protocols utilize a 2 hour time point at 37°C (mimicking physiological conditions), but we chose to examine both 37°C and room temperature (~25°C); incubating for 30 minutes, 1 hour, and 2 hours.

Comparing the results of these activations with the standard fluorogenic substrate FS-6 (Sigma) activity assay, it was observed that both human and murine MMP-9 activated at room temperature displayed a higher level of activity than that of MMP-9 activated at 37°C. Moreover, the activities seen (Figure 14 A, B) all clustered tightly based on their incubation temperature, without a dependence on time.

To further confirm these results, protein gels were run on the pro (stock and biotinylated) and activated forms of MMP-9, comparing both the incubation conditions of duration and time (Figure 14C), and the stability of the activated MMP after storage at 4°C (Figure 14D). Examining the results, the activated protein demonstrated a consistent decrease in size compared to the pro forms of MMP-9, similar to what would be expected with pro-peptide domain cleavage. Comparing the incubation temperatures and time points, it is clear that incubation at 37°C results in greater degradation of the MMP, as does extending the time of incubation (Figure 14C), further confirming our protocol (fully described below in Experimental Methods Section 2.6). Additionally, the activated protein stored at 4°C for 3 days displayed signs of advanced degradation (Figure 14D), indicating that MMP should be freshly activated for each use.

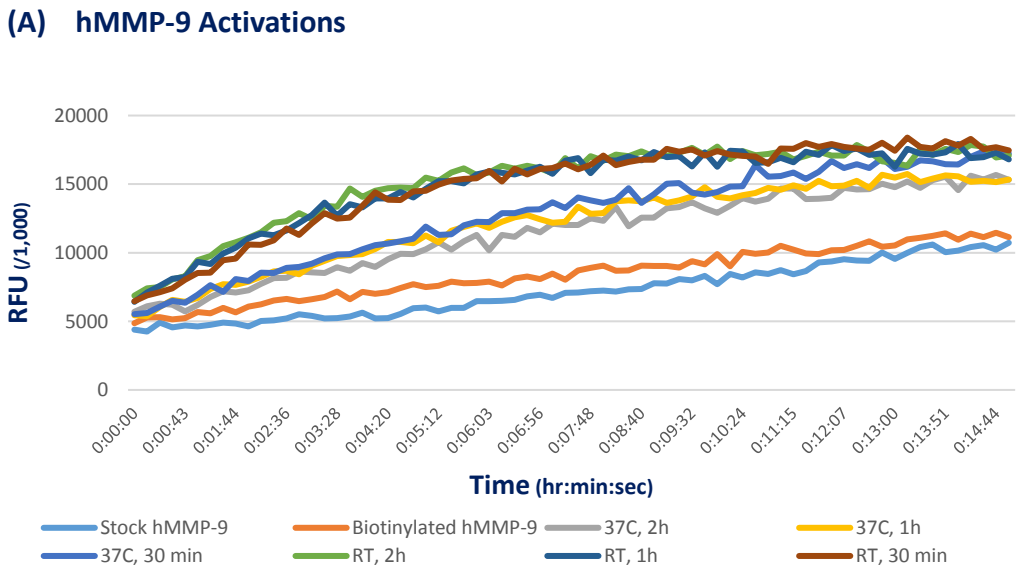

(B) mMMP-9 Activations

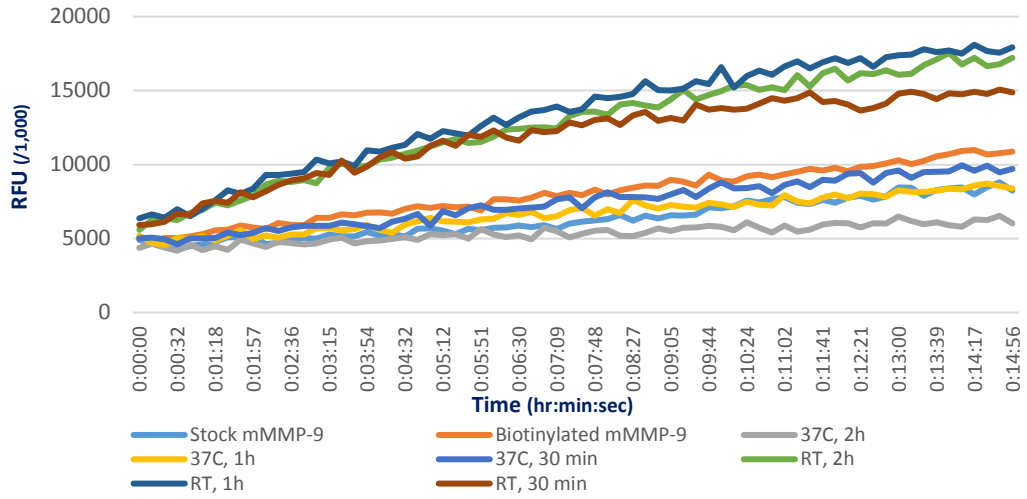

(C) hMMP-9 Activation (37°C v RT)

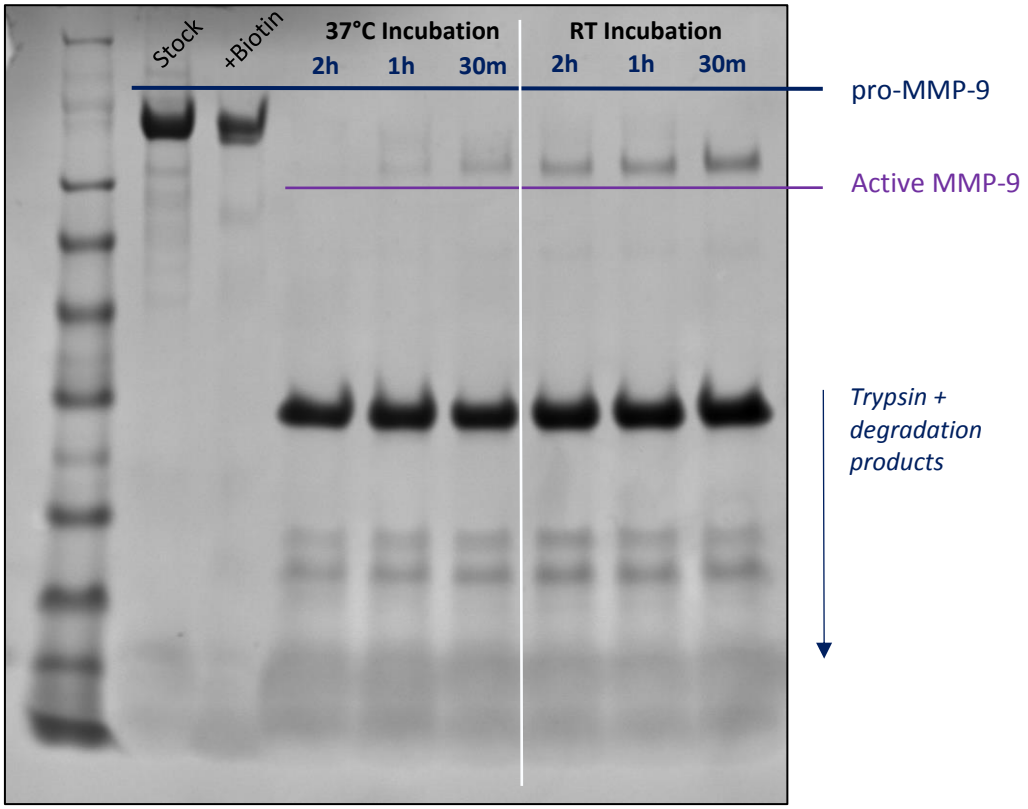

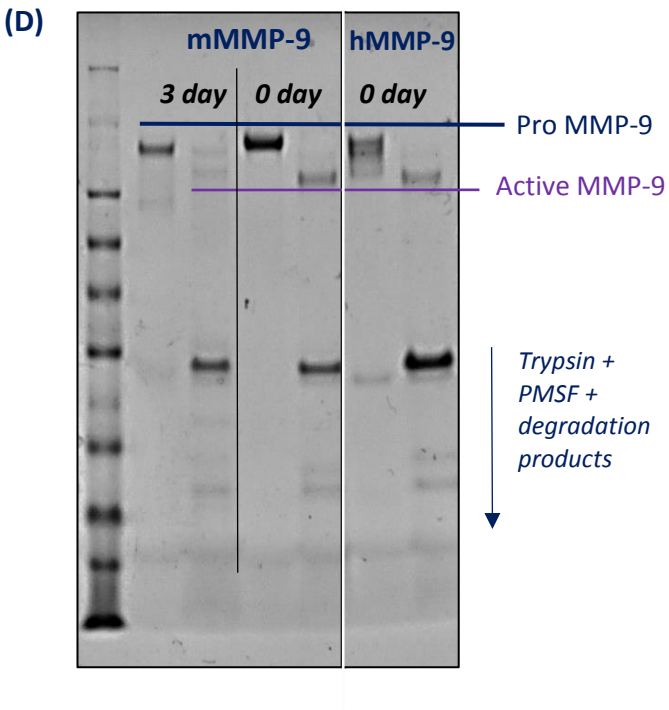

Figure 14. Benchtop Activation Validation

(A, B) Readouts of MMP-9 activity using fluorogenic substrate FS-6, comparing incubation time and temperature.

(C) Protein gel corresponding to the activations seen in (A).

(D) Protein gel corresponding to the activation results in (A) and (B), examining protein degradation over time.

All activations employed the following: MMP-9 (1 mg/mL) + Trypsin (0.5 mg/mL) + Activation Buffer 5(0 M Tris-HCl, 150 mM NaCl, 5 mM $CaCl_2$), in a ratio of 1:2:7. The trypsin cleavage reaction was quenched using 100 mM PMSF.

2.2.2. MMP-9 Single Clone Binders

With the activation protocol established, we turned to validating previously patented (Dyax Corporation)[67] MMP-9 single clone binder M0076 and inhibitor DX-2802 (Section 2.1.5).

The patent states that both clones bind the human and murine forms of MMP-9, while DX-2802 binds selectively to the active form of the protein and displays inhibitive properties. By comparing binders and inhibitors isolated from the CDR-H3 and Sidhu Libraries with these previously characterized single clones, we could further validate this method of selection. The difference in binding and inhibitive properties of M0076 and DX-2802 also could be further utilized to develop an assay comparing binding versus inhibition of isolated proteins displayed on the yeast cell surface.

To analyze single clone binders M0076-D03 and DX-2802, flow cytometry experiments were performed with both the pro and active forms of both human and murine MMP-9 isoforms and incubated at concentrations between and including 50 and 250 nM for standard 30 minute primary labeling, as well as through time course experiments for 1 – 6 hours at each hour. The time course experiments were employed to confirm biding versus inhibition of the active MMP-9 over an extended period of time, to ensure that the single clones are able to resist cleavage by the active form of the protein.

2.2.2.1. Pro v. Active MMP-9 Binding

As stated in the patent, the results of pro versus active binding flow cytometry experiments (2e6 cells per sample, 50 nM, 30 minute primary incubation; Figure 15) demonstrate that DX-2802 binds preferentially to the active, human isoform of MMP-9 with little to no binding of the pro human or murine isoforms. M0076, however, shows clear binding to both the pro and active forms of human MMP-9.

Contrary to expectations, neither clone displayed significant binding to either pro or active murine MMP-9 (Figure 15 A, B), at 50 nM, 100 nM, or 200 nM. But, when binding experiments were repeated using protein that was stored at 4°C for 3 weeks, substantial murine MMP-9 binding was observed (Figure 15 C), as stated in the patent. Storage of MMP-9 at 4°C for greater than approximately 10 days results in significant protein degradation, suggesting that the clones may be binding to a site exposed by a more degraded form of the murine MMP-9 protein. While further validation of this result is required (perhaps utilizing circular dichroism – in combination with the flow cytometry and protein gels – to more directly visualize MMP-9), it suggests that these single clones preferentially bind a more degraded form of murine MMP-9. Given the inconsistency of the murine MMP-9 binding observed, future experiments with M0076 and DX-2802 focused solely on the human MMP-9 isoform.

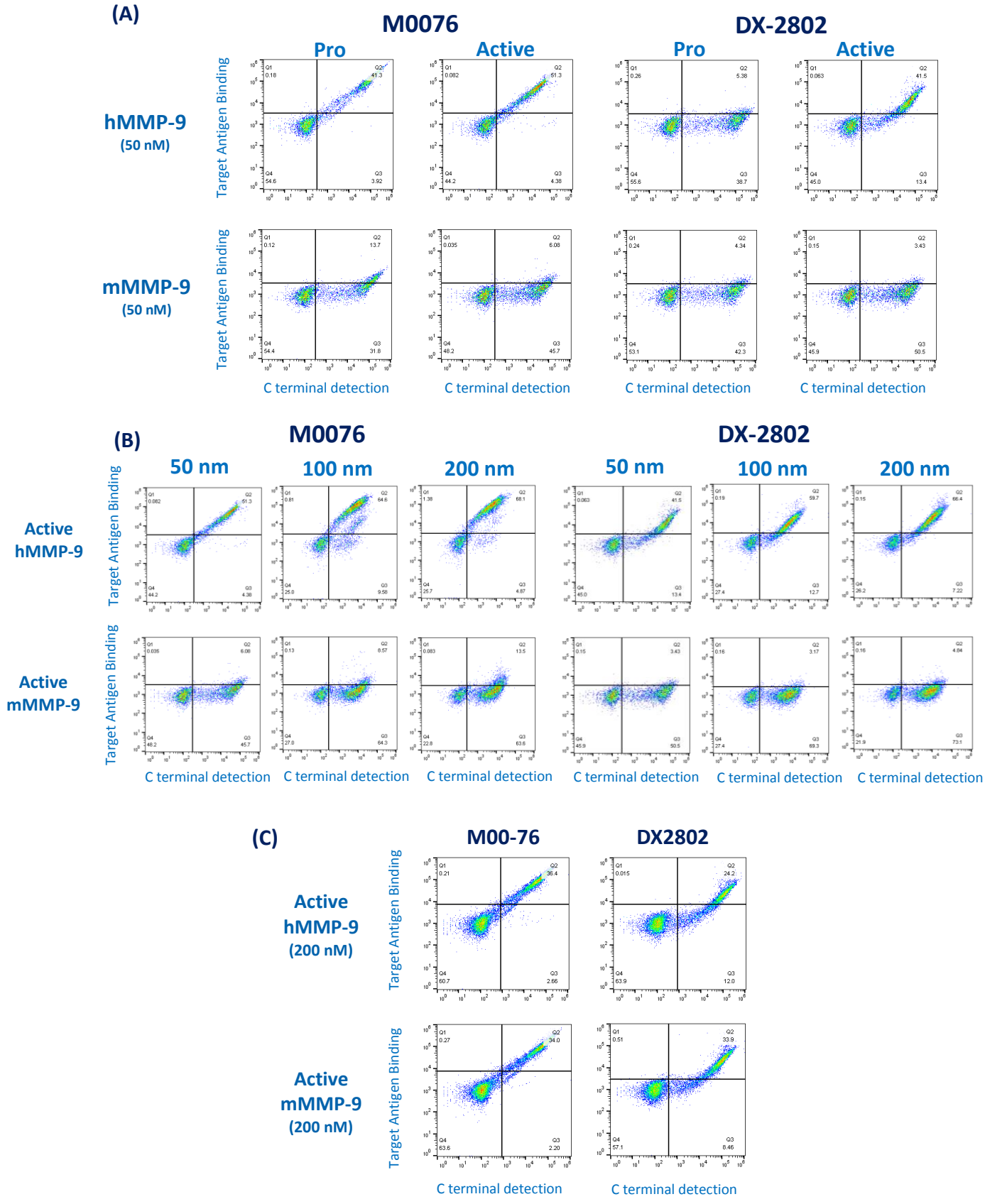
(A)
M0076
DX-2802
Pro
Active
Pro
Active
hMMP-9
(50 nM)
mMMP-9
(50 nM)
Target Antigen Binding
C terminal detection
(B)
M0076
DX-2802
50 nm
100 nm
200 nm
50 nm
100 nm
200 nm
Active
hMMP-9
Active
mMMP-9
Target Antigen Binding
C terminal detection
(C)
M00-76
DX2802
Active
hMMP-9
(200 nM)
Active
mMMP-9
(200 nM)
Target Antigen Binding
C terminal detection

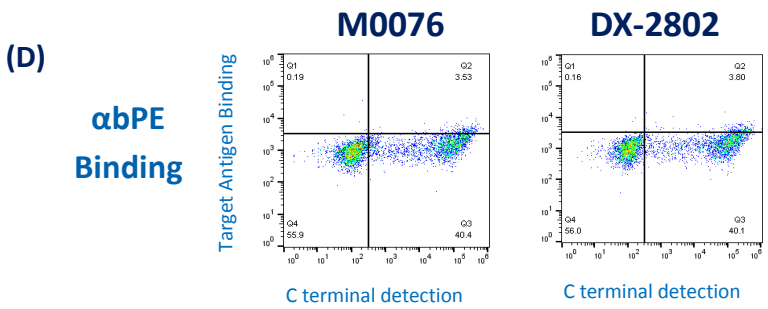

Figure 15. Initial M0076 and DX-2802 Characterization

(A) Displays pro versus active binding of human and murine MMP-9, confirming that DX-2802 preferentially binds to active hMMP-9, and neither clone binds well to murine MMP-9. **(B)** Compares binding of both clones to increasing concentrations of MMP-9 at 50, 100, and 200 nM. The binding profile begins to shift left and becomes broader/less distinct as the concentrations increase, indicating that MMP-9 is having an enzymatic cleavage effect. **(C)** In this experiment, human and murine MMP-9 that had been stored for 3 weeks at 4°C was used. **(D)** A lack of observed vertical shift confirms that neither clone binds to the fluorescent, secondary label anti-biotin PE, ensuring that binding observed is solely due to MMP-9 binding to the clones.

2.2.2.1. Time Course Characterization

With the initial validations of M0076 and DX-2802 completed, we attempted to utilize these known binder and inhibitor proteins to develop a strategy to distinguish between isolated protein candidates for binders, versus inhibitors. Our solution to this was time course experiments. Time course experiments extend the standard flow cytometry and assay incubations of binding protein and MMP target from 30 minutes, to 6 hours; with measurements taken at 30 minutes, and each hour on the hour (Figure 16). Experiments otherwise followed the standard protocol, using 50 nM human MMP-9, and 2e6 cells/sample. In the final resuspension time course experiments (Fig. 16 C), single clones were incubated for 30 minutes with activated, human MMP-9 before being washed of excess MMP-9, resuspended, and allowed to incubate for the remaining time span, up to 6 hours.

The active form of human MMP-9 demonstrated cleavage on M0076 and DX-2802 displayed on the yeast cell surface, resulting in visible truncation on the single clone binders at higher concentrations of 100 nM and 200 nM during standard primary incubations of 30 minutes (Fig. 15 B). When further exploring this truncation with time course experiments (Figure 16 A, B), both clones saw cleavage when incubated with 50 nM activate, human MMP-9 for 6 hours. This reveals that, under these conditions, even an Ab with reported inhibitory characteristics does not completely inhibit MMP-9 cleavage when displayed on the yeast surface.

Resuspension time course experiments were then performed to test whether the cleavage seen was a result of excess MMP-9 in solution, or more directly tied to binding of the Ab against the MMP. Interestingly, DX-2802 demonstrated significantly greater truncation than M0076, even after 6 hours. This suggests that M0076 is binding MMP-9 at a distance from the active site, and so is able to avoid cleavage once excess MMP is removed from solution. By contrast, DX-2802 binds only the active form of MMP-9, indicating that it does so at a site closer to or within the active site of protein, once the pro-peptide domain is removed. As such, while the exact cause is uncertain, the cleavage observed may be the result of binding near, but not within the active site of MMP-9. This would ensure specific binding against only the active form (once the pro-peptide domain is removed), and provide a physical blockage of the active site to serve an inhibitive effect. Over time, however, the protein binder may itself be cleaved by this proximity to the active site. No matter the reason, this suggests that, despite inhibition observed, DX-2802

remains susceptible to the enzymatic activity of human MMP-9, highlighting once again the need for improved protein inhibitors.

Knowing the properties of these binder and inhibitor proteins against pro and active MMP-9, we can now attempt to develop a binding versus inhibition assay, to enable more rapid and comparative characterization of isolated MMP-9 binders on the yeast surface (Section 2.2.3). We also have a baseline of comparison for protein binders isolated from the CDR-H3 and Sidhu Libraries.

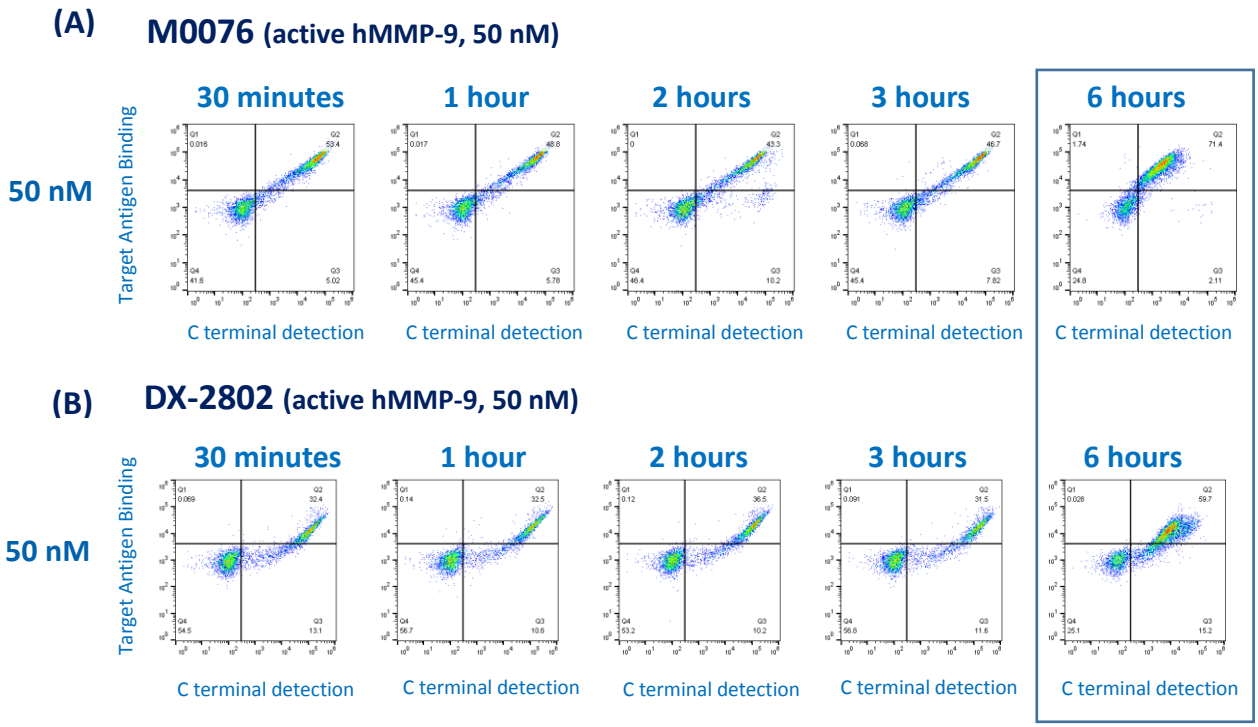

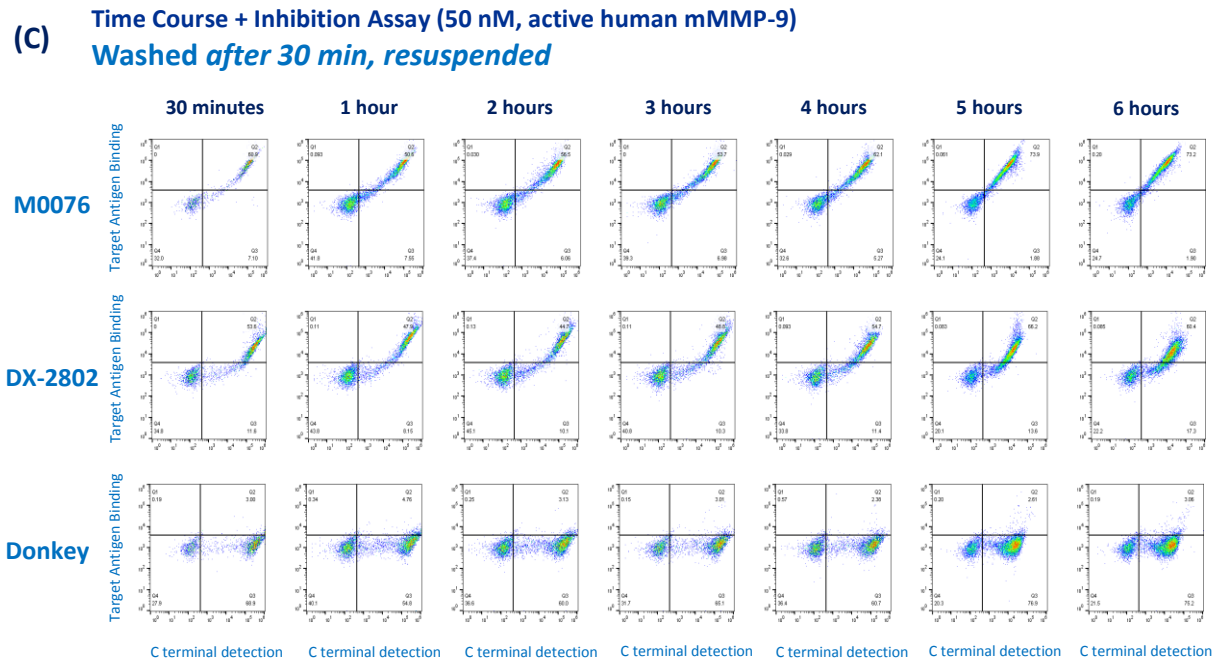

Figure 16. Time course experiments

Initial: 50 nM human MMP-9; 30 min – 6 hours, 2e6 cells/sample. **(A)** M0076 **(B)** DX-2802. By the 6 hour time points (boxed) the active MMP-9 has begun to cleave both binding clones. This can be seen from the left shift and widening populations in Q2 in both M0076 and DX-2802, as these changes are indicative of protein truncation. **(C)** Resuspension: 50 nM human MMP-9; 30 min incubation, wash, resuspend for varying time points up to 6 hours; 2e6 cells/sample. A Donkey IgG binding clone is used as a negative control.

2.2.3. Yeast Display Inhibitor Assay: Development and Single Clones

Development of the yeast display inhibitor assay employed single clone MMP-9 binders M0076 and DX-2802 as positive controls for binding and inhibition, as well as single binding clones against Donkey IgG isolated from the CDR-H3 Library as a negative control. The assay mirrored flow cytometry primary labeling, incubating MMP-9 with individual cell samples. Upon completion of incubation, cells were washed of excess MMP-9, resuspended, and fluorogenic substrate FS-6 was added before running the samples on a plate reader, using the same settings as the MMP-9 activity assay (Section 2.4.5) for timing, excitation, and emission. Baseline experiments focused on establishing sample volume, FS-6 concentration, number of cells per sample, MMP-9 concentration, run time per experiment, and relative fluorescence unit (RFU) readout ranges and curve standards. Once baseline experiments were completed, the assay was paired with time course experiments as a second test of inhibition over time.

2.2.3.1. Baseline Experiments

Using the MMP-9 and Donkey scFv-binding displayed cells, baselines were established against a wide range of FS-6 (1x, 5x, 50x, 100x, 200x) and pro and active MMP-9 concentrations (50 nM, 100 nM, 200 nM), both with and without cells (testing 500,000, 2e6, and 10e6 cells/sample). Through these experiments, standards of: 50x FS-6, 100nM MMP-9, and 2e6 cells per sample (15 minutes run time) were established. Reviewing MMP-9 activations, it was consistently observed that the verification readout plateaus at ~2e7 RFU when run with 50x FS-6 (Fig. 17A). It was also observed from the baseline inhibition assay tests that the

baseline readout of experiments with the combination of cells, FS-6, and inactive MMP-9, ranges between approximately 400,000 – 600,000 RFU (Fig. 17B). While these results were consistent across experiments performed for this work, it is important to note that they remain "relative" fluorescence intensity values, and so are dependent on the settings of the plate reader and experiment.

With baselines established, experiments for the assessment of binding versus inhibition were then performed, combining, the varied concentrations of FS-6 and active MMP-9 with the number of cells described above. Examining Figure 17C, we see little difference with the addition of 50 nM MMP-9, but a potentially slight increase in the response of the M0076 incubated with active human MMP-9. Repeating the experiment with increased concentrations of MMP-9 (100 nM, 200 nM; Figure 17D), we can more clearly see the difference between the responses of the three single clone binders. The negative, donkey IgG binders do not result in FS-6 cleavage, indicating that the MMP-9 added during labeling was removed during the washing steps.

Comparatively, samples containing M0076 and DX-2802 demonstrate clear FS-6 cleavage corresponding to active MMP-9 in the samples, though no significant difference was noted for either 100 nM or 200 nM MMP-9, and so 100 nM was chosen for the protocol. While the activity observed is greater for M0076 than DX-2802, this follows what might be expected from the flow cytometry characterizations, from which we postulated that M0076 binds MMP-9 outside of the binding site, while DX-2802 demonstrates partial inhibition of the enzyme. As

such, while further development is required, we establish the possibility of distinguishing between binders versus inhibitors of active MMP-9.

(A)

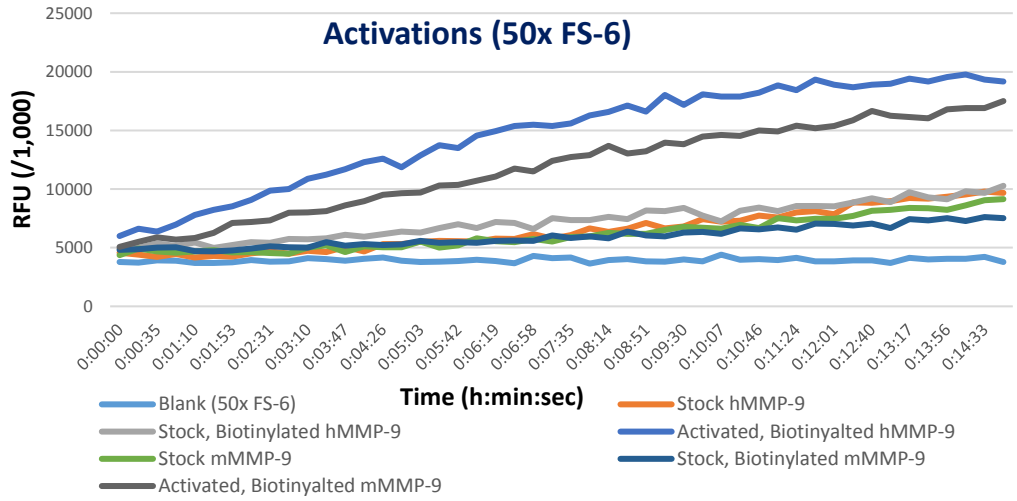

(B)

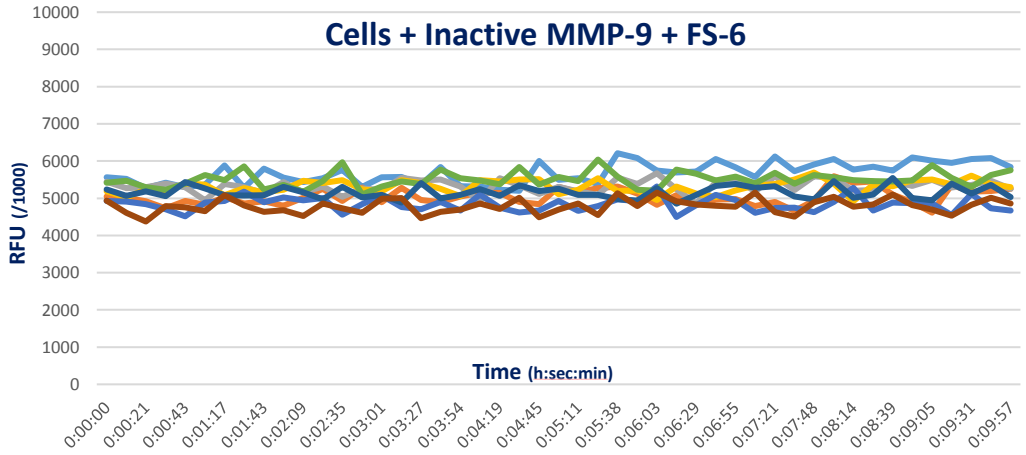

(C)

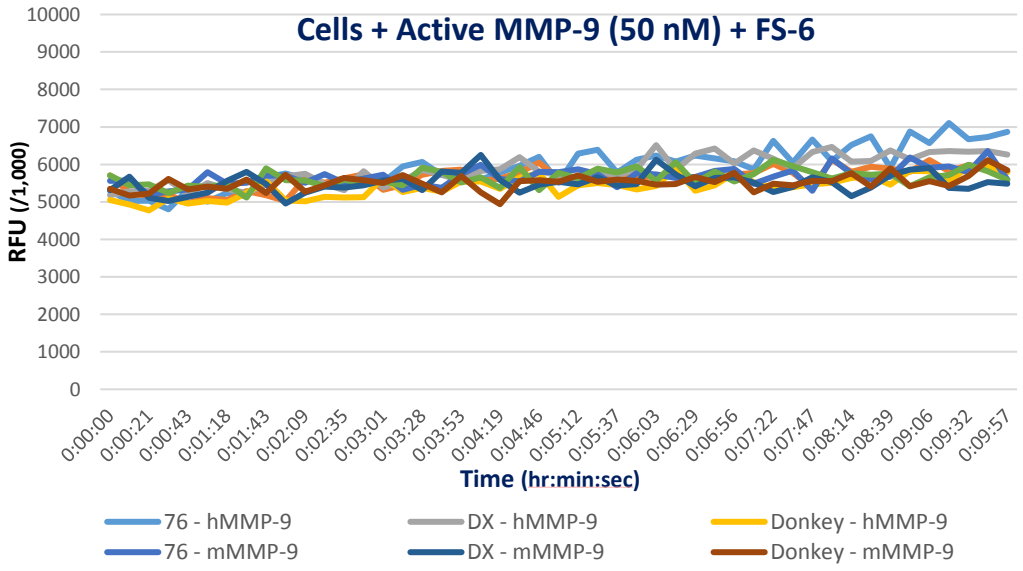

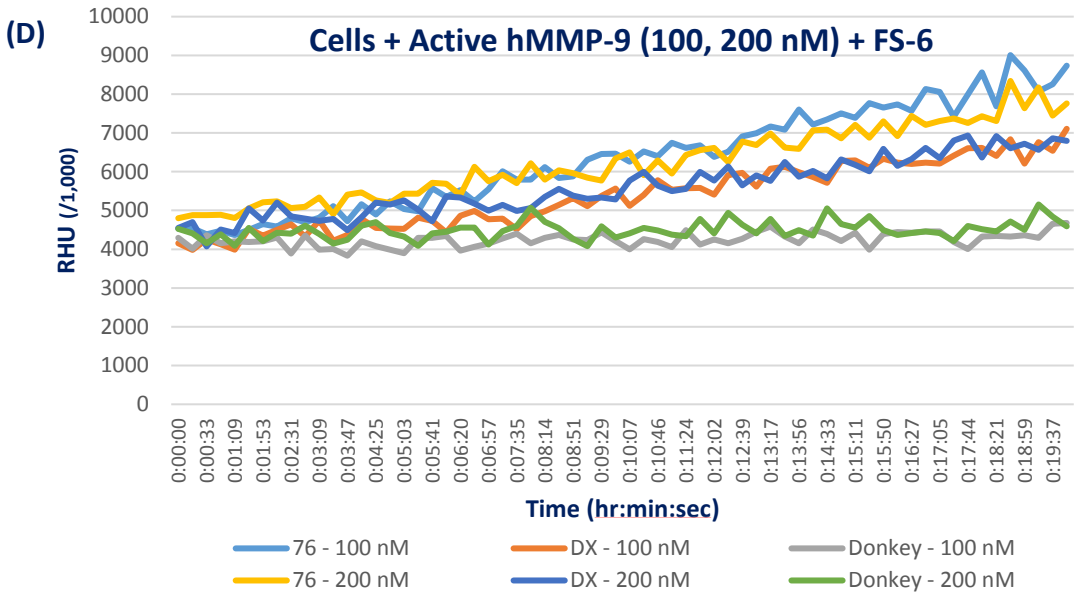

Figure 17. Baseline Inhibition Assay Experiments (50x FS-6, 50 nM MMP-9) **(A)** Activations. **(B)** Biotinylated MMP-9 with cells and FS-6, **(C)** Activated MMP-9 (50 nM; washed at the end 30 min incubation), samples with cells and FS-6, **(D)** Activated MMP-9 (100, 200 nM; washed at the end 30 min incubation), samples with cells and FS-6. Examining (C & D), it is clear that M0076 and DX-2802 have a substantial but imperfect binding effect on the active MMP-9, as there is some release of the active MMP-9 for it to cleave the fluorogenic substrate.

2.2.4. MMP-9 Binder Isolation

Isolation of MMP-9 binders was performed against two synthetic, yeast display protein libraries, neither of which was designed for the inhibition of proteinases, the CDR-H3 and Sidhu Libraries.

2.2.4.1. CDR-H3 and Sidhu Libraries

Magnetic bead sorting (MBS) was used to enrich the populations of both libraries against single track, and alternating track isoforms of MMP-9. MBS against the Sidhu Library was performed using Biotin Binder DynaBeads (Thermo Scientific), while sorting against the CDR-H3 Library used M-270 Streptaviding DynaBeads (Thermo Scientific), to ensure that the process was not bead dependent. The Sidhu Library was further enriched using FACS after the third round of sorting, while the CDR-H3 Library employed magnetic bead sorting through six rounds before isolating single clones directly from the enriched populations without performing FACS. With each round, flow cytometry was used to ensure proper induction for full-length scFv expression; 2e6 cells per sample were labeled at 50 nM antigen during 30 minute primary incubation; and single color controls and 10,000 events per sample collected by the flow cytometer ensured consistency between experiments.

2.2.4.2. Sidhu Library: MMP-9 Enrichment and Characterization

Through magnetic bead sorting, the initial population was suitably enriched within three rounds to ensure a significant population of binders against active,

human and murine MMP-9. We then switched to FACS to ensure isolation of as many clonal variants as possible, as some clones may be lost between rounds of magnetic bead sorting. Examining the population isolated after FACS, we observe that there appears to be cells binding highly variable amounts of MMP-9 as compared to single clones M0076 or DX-2802, suggesting clonal diversity.

2.2.4.3. CDR-H3 Library: MMP-9 Enrichment and Characterization

Using magnetic bead sorting, the CDR-H3 Library was sufficiently enriched within six rounds of alternate isoform sorting to ensure a significant population of cross-reactive binders against active, human and murine MMP-9 (Figure 20). Interestingly, the population was first strongly enriched against the human isoform, before a final sort thereafter enriched the population strongly against murine MMP-9. Examining the enriched population of binders (Fig. 20 A), we see that there is a broad spread of potential binders, again indicating clonal diversity and binders of varying strength.

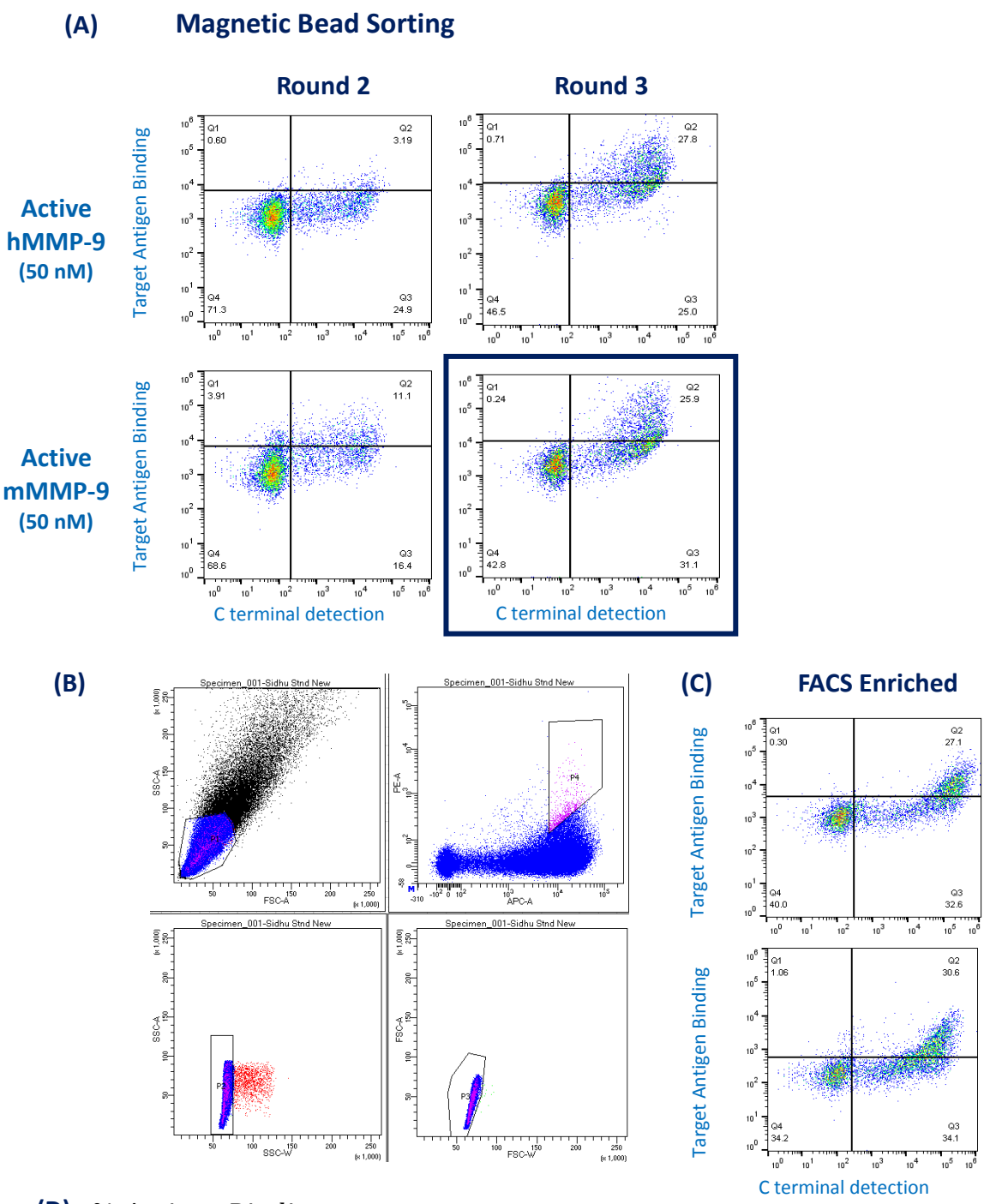

(D) $\%\ Antigen\ Binding$

$$Human\ MMP-9\ \left(\frac{27.1}{27.1+32.6}\right) * 100 = 45.4\%$$

$$Murine\ MMP-9\ \left(\frac{30.6}{30.6+34.1}\right) * 100 = 47.3\%$$

Figure 18. Sidhu Library Magnetic Bead Sorting and FACS

(A) Magnetic Bead Sorting Enrichment – Flow Cytometry, **(B)** FACS Setup, **(C)** FACS Enrichment – Flow Cytometry, **(D)** Percent Antigen Binding

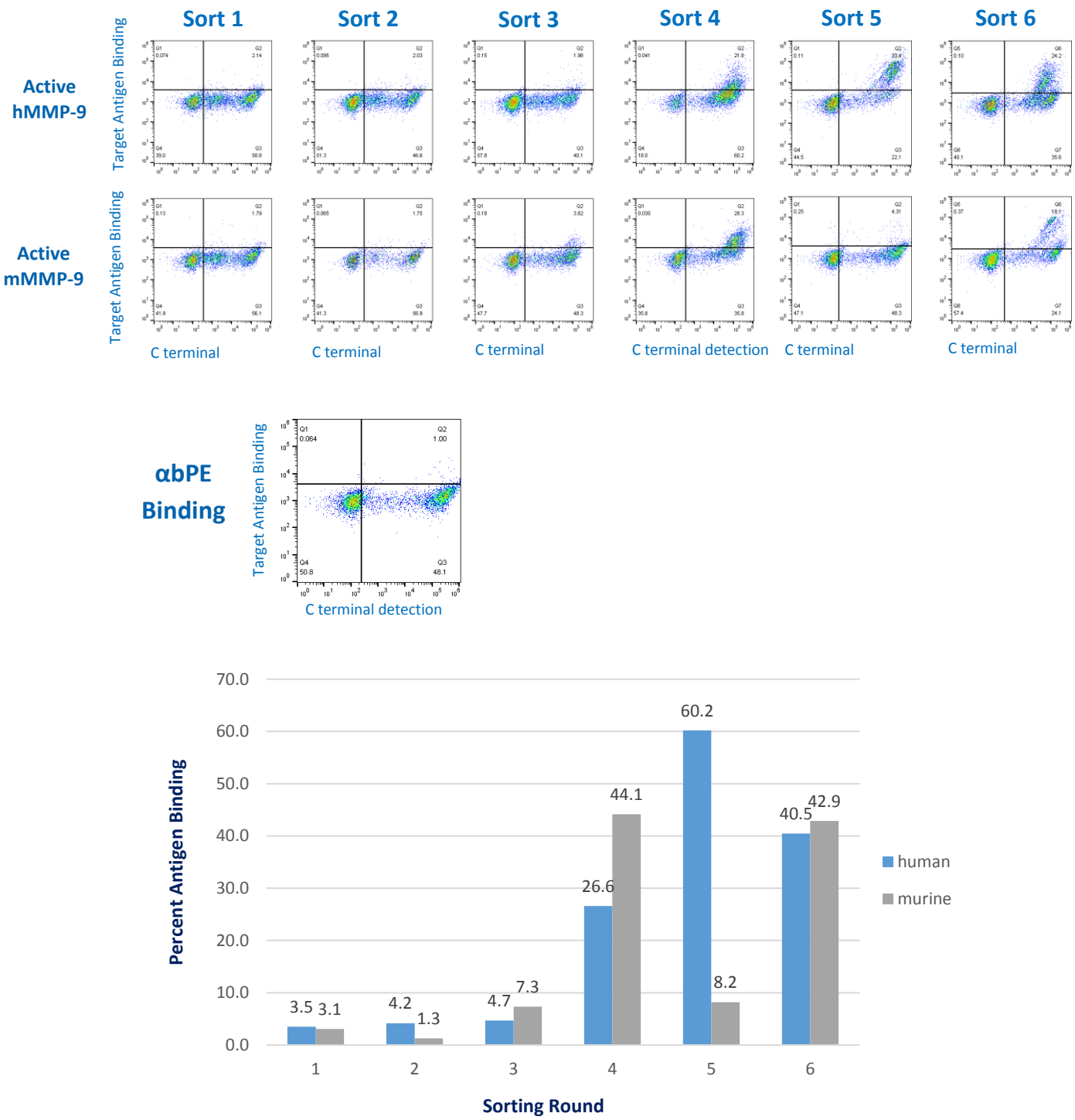

Figure 19. Magnetic Bead Sorting Enrichment – beginning with hMMP-9 and alternating with mMMP-9, Rounds 1-6

(A) Flow Cytometry with anti-biotin PE check, **(B)** Percent Antigen Binding

2.2.5. Further Characterizing the CDR-H3 Library: Donkey IgG

To further assess the newly designed and created CDR-H3 Library, binding proteins against Donkey IgG – a standard library construction assessment protein – were isolated and characterized. As with the MMP-9 sorts, magnetic bead sorting using M270 Dynabeads was employed to enrich the library for binders. Given the successful isolation of binders against two diverse proteins – Donkey IgG and MMP-9 – we can begin to say that the CDR-H3 Library has proven successful for the isolation of protein binders.

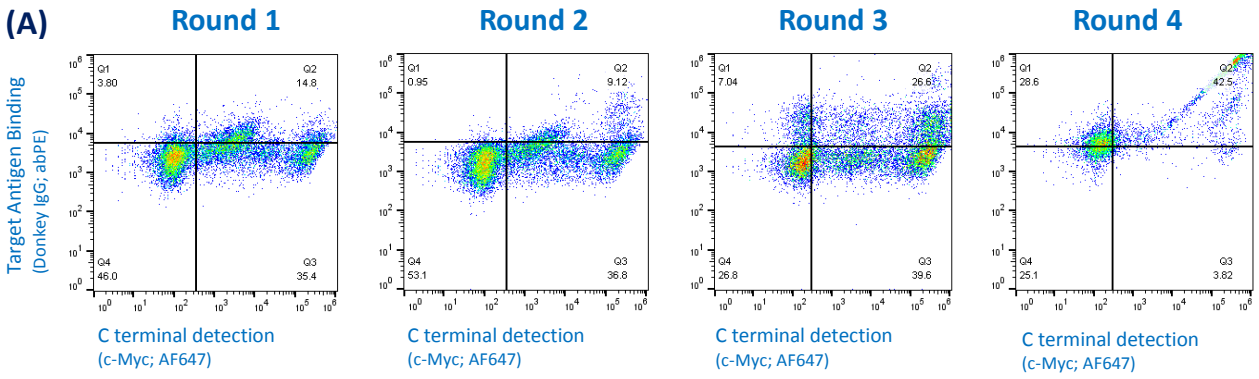

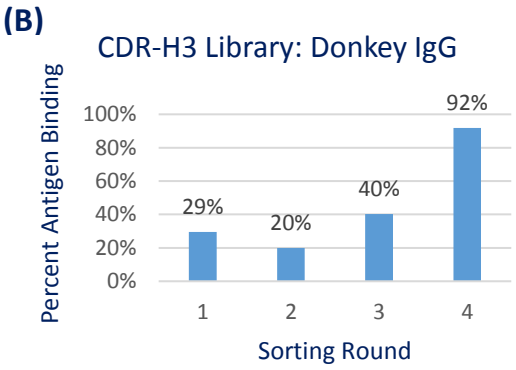

Figure 20. Donkey IgG Enrichment **(A)** Flow cytometry data. Rounds 1-3 contain two regions of enrichment, the left of which corresponds to the enrichment of truncated proteins. By Round 4, however, enrichment has shifted to full-length binders, as can be seen by the single, tight population in Q2. **(B)** Corresponding Percent Antigen Binding

2.3. Conclusions

Protocols for the benchtop activation of MMP-9 and to examine the binding versus inhibitive effects of yeast displayed MMP-9 binders were established. Cross-reactive binders against human and murine MMP-9 were enriched for and isolated from both the Sidhu and CDR-H3 Libraries, neither of which was expressly designed for enzymatic binder isolation. In doing so, two bead types were utilized to ensure the robustness of the method. With the isolation of these binders, single clone isolation, sequencing, subcloning, and titration experiments for characterization are the next steps in this work. These results not only validate the spatially limited diversity design of the CDR-H3 Library, but provide a template for expanded design of mini-libraries which incorporate noncanonical amino acids at various positions to facilitate protein-small molecule hybrid screening and isolation, furthering the development of highly specific and selective PSMHs for tool compound use and therapeutic development.

2.4. Experimental Methods

2.4.1. Cell Culture

2.4.1.1. Media Preparation, Standard Bacterial and Yeast Cell Culture

Procedures for the preparation of liquid media and media plates; and DNA isolation from and transformation into *E.coli* and yeast were performed as previously described[46,73]. All experiments used the *E.coli* strain DH5αZ1 and the yeast strain RJY100, which was constructed by homologous recombination as described in detail elsewhere[46].

2.4.1.2. Yeast Display Library Frozen Stock Preparation

The yeast display library of 1 x 10^9 clones was inoculated in 1L SD-CAA (-Trp, -Ura) and incubated with shaking at 30°C, 300 RPM overnight to saturation at 20 times the number of transformants, as determined by plating and optical density (OD_{600}) measurements. Once saturation was reached, 10 times the number of transformants were spun down (5 minutes, 2,000g, 4°C), and evenly divided to be resuspended in 8L SD-CAA (-Trp, -Ura). Upon reaching saturation once more, the cells were spun down, washed, resuspended in 15% glycerol, and frozen in 1.5 mL aliquots at -80°C to form master stocks.

2.4.1.3. Yeast Display Library Propagation, Induction, and Sorting

A yeast display library of 1 x 10^9 clones is inoculated in 1L SD-CAA (-Trp, -Ura) using two master stock vials from -80°C, and grown to saturation overnight at 30°C, 300 RPM. The library is then passaged to an OD_{600} of 1, and re-grown to

saturation. At this time, as per the OD_{600} measurement, a portion of the culture was saturated to propagate the culture to an OD_{600} of 1, while the remainder is placed at 4°C to form a fridge stock; library fridge stocks remain viable for 1 month. The propagated culture is grown to reach exponential growth (mid-log phase, OD_{600} 2-5), and then pelleted (5 minutes, 2,000g, 4°C). The cells are resuspended to an OD_{600} of 1 in SG-CAA (-Trp, -Ura) induction media, and grown at 20°C (to facilitate protein production) for at least 12, but preferably 16-20 hours. Once induced, the library is pelleted, washed three times with ice-cold, 1x PBSA (pH 7.4), and resuspended in 5 mL ice-cold, 1x PBSA (pH 7.4) to prepare for magnetic bead sorting.

2.4.1.4. Mammalian Cell Culture and Transfection

Suspension culture mammalian HEK293-F cells were kept between 0.3 x 10^6 and 3 x 10^6 million cells/mL by passaging by dilution every 3 days into fresh Freestyle medium (Life Technologies). Cells were incubated at 37°C, 8% CO_2, 125 RPM. Four or more passages were performed prior to transfection approximately 24 hours after seeding the cells at 0.5 x 10^6 cells per mL, using polyethylenimine in FreeStyle 293 media supplemented with OptiPro (Life Technologies). Cells were incubated (37°C, 8% CO_2, 125 RPM) for 6-8 days before protein harvesting.

2.4.2. Protein Preparation

2.4.2.1. Construct Preparation

Human and murine isoforms of MMP-9 were expressed through transfection of the aforementioned HEK293-F cells. Human and murine MMP-9

pCMV-ORF-His expression constructs were purchased from Sino Biological[74,75]. Constructs were sequenced (Eurofins) to ensure correct assembly, and maxiprepped from transformed DH5αZ1 *E.coli,* grown with kanamycin, for transfection into HEK-293F cells as described in section 1.2.2.1.4.

2.4.2.2. Protein Purification

6-8 days after transfection, the culture was harvested, cells filtered for supernatant-containing target protein, and supernatant pH-adjusted with 10x phosphate-buffered saline (PBS). Protein A resin (Genscript) was used to purify the Fc fusion proteins DPP-IV and FAP, while Ni-NTA resin (Genscript) was used to purify MMP-9, following recommendations of the manufacturer. Concentrations of the eluted proteins were measured, protein gels run to ensure purity, and aliquots of 0.5 mg/mL were prepared in 50% glycerol (vol/vol) and flash frozen using liquid nitrogen for freezing prior to storage at -80°C. Enzymatic activity of the proteins was also confirmed, using the fluorogenic substrate FS-6 (Sigma) for MMP-9, and fluorogenic substrate Ala-Pro-7-amino-3-trifluoromethylcoumarine (Calbiochem) for DPP-IV and FAP.

2.4.2.3. Chemical Biotinylations

To prepare chemically biotinylated proteins from frozen or refrigerator protein stocks, EZ-Link NHS-LC-Biotin (ThermoScientific) was used. Frozen stocks of MMP-9 were rapidly thawed in room temperature water, and then buffer exchanged into 1x phosphate-buffered saline (PBS; pH 7.4) using Amicon Ultra-

0.5 30 kD MWCO devices, for storage at 4°C for up to 2 weeks. Donkey IgG was stored at 4°C indefinitely. Chemical biotinylations were then performed using EZ-Link NHS-LC-Biotin (Thermo Scientific) with targeted biotinylation levels of 1-2 biotins per protein, verified using the Pierce Biotin Quantitation Kit (Thermo Scientific), and stored at 4°C for one week (previously frozen enzymes) or indefinitely (all others).

2.4.3. Magnetic Bead Sorting

Magnetic bead sorting was performed according to previously described methods[73], summarized as follows. Initial library inoculation, propagation, induction, and preparation were performed as described in Section 1.2.1.3, at which time the cells were incubated with 50 µL of antigen-coated magnetic beads, on a rotary wheel for 2 hours at 4°C. Cells bound to the magnetic beads were drawn from solution, washed once with ice-cold PBSA, and placed in 50 mL SD-CAA (-Trp, -Ura) for overnight growth at 30°C, 300 RPM. Once mid-log phase was reached, cells were spun down (5 minutes, 2,000g, 4°C), resuspended and incubated briefly against the magnet, and cells not bound to the magnetic beads passaged to a 100 mL SG-CAA (-Trp, -Ura) induction culture for overnight growth (20°C, 300 RPM) to repeat the process, this time using 10 µL of antigen-coated magnetic beads. Rescued and induced population samples were stored at 4°C. Flow cytometry was used as described below to detect the fraction of displaying cells that bind the target of interest – calculated and reported as percent antigen binding – and this process is repeated until a sufficient degree of enrichment has occurred.

Depletion sorts (also called negative sorts) against streptavidin, biotin, and TA99 (murine Fc; as in DPP-IV and FAP fusion proteins) were also performed against the CDR-H3 and Sidhu Libraries to ensure binders were not being isolated against non-targets. With the Sidhu Library, these sorts were performed during the first, third, etc. rounds; with the CDR-H3 library, these sorts were performed on round three, five, etc. as the stock library was previously depleted against the potential aforementioned negative selection targets.

2.4.4. Flow Cytometry

All flow cytometry experiments reported here were performed using standard protocols[73]. Full-length expression and induction were assessed using simultaneous detection of the N- and C- termini epitope tags, HA and c-Myc respectively (primary labels – 1:500), using goat-anti mouse Alexa Fluor 488 (AF488) and goat anti-chicken Alexa Fluor 647 (AF647; Life Technologies) as the respective, fluorescent secondary labels (secondary labels – 1:500). During antigen-binding experiments, the c-Myc tag was detected as described, while the target was detected using appropriate concentrations of antigen (standard, 50 nM) during primary labeling, and (1:500) streptavidin AF488 or anti-biotin PE during secondary labeling, utilizing the greater than 1 biotin/protein biotinylation average.

2.4.4.1. Fluorescence Activated Cell Sorting (FACS)

Labeling for FACS followed the same methodology as for standard flow cytometry and employed the Tufts Core Sorting Facility at the Tufts Medical School. All

samples were prepared prior to transport, spun down, and stored on ice until resuspension immediately prior to sorting.

2.4.5. Benchtop MMP-9 Activation and Verification

Activation of MMP-9 was performed using trypsin (0.5 mg/mL) to cleave the pro-domain during a 30 minute incubation at approximately 25°C (room temperature), with the following volume ratio: (1) MMP-9 (1 mg/mL), to (2) Trypsin (0.5 mg/mL), and (7) Activation Buffer. Activation buffer consists of 50 M Tris-HCl, 150 mM NaCl, and 5 mM $CaCl_2$. Once the incubation was completed, the trypsin cleavage was quenched using 100 mM PMSF, adding the same volume as the added MMP-9. Activation of the protein is verified by observing and comparing the rates of reaction of pro- and active-MMP-9 using a plate reader to record the readout of the cleaved the fluorogenic substrate FS-6 (50x), resuspended in TCN buffer (50 mM Tris base, 10 mM $CaCl_2$, 0.15 M NaCl; pH 7.5), with 50 uL per sample, measured every 10 seconds for 15 minutes (excitation – 323 nm, emission – 398 nm).

2.4.6. MMP-9 Time Course Experiments

Time course experiments followed the same primary labeling as flow cytometry and FACS, but extended the incubation time; instead of the standard 30 minutes, incubations were completed for up to 6 hours, taking time points at each hour (30 min, 1h, 2h, 3h, 4h, 5h, 6h). In addition, c-Myc was not added until the

last 30 minutes of sample incubation. As described, time course experiments were used to assess single clone binding resistance to MMP-9 cleavage over time.

2.4.7. Clonal Isolation and Characterization

2.4.7.1. Library Enrichment

All sorts were performed using coverages of at least 10 times the expected library or population size. Magnetic bead sorts were performed using Dynabead Biotin Binder Beads (Life Technologies) or M270 Beads (Life Technologies). Alternating rounds of bead sorting including two negative sorts against streptavidin (using just the streptavidin-coated magnetic beads) and biotin, followed by a positive enrichment against the antigen target. Sorting progress was monitored via flow cytometry. To ensure enrichment of cross-reactive binders to human and murine isoforms of MMP-9, two tracks per sort were started, and each round of magnetic bead sorting alternated the isoform sorted against: the first round was completed with the human isoform, the second with the murine isoform, and so on; with each sort, the isoforms enriched against would alternate as shown below:

Alternating Tracks

Track 1: human → murine → human → murine →

Track 2: murine → human → murine → human →

Figure 21. Alternating isoform tracks for MMP-9 binder isolation using magnetic bead sorting

2.4.7.2. Single Clone Isolation

Final populations were zymoprepped, transformed into *E.coli* and plated on solid media containing ampicillin. Colonies were picked, miniprepped, and sequenced (Eurofins). Genetic analysis was performed using Geneious to examine sequences for areas of variability as compared to the original antibody and the planned CDR mutations. Sequence selected clones were then transformed into back RJY100 using the Frozen-EZ Yeast Transformation II Kit (Zymo Research), for further characterization.

2.4.7.3. Characterization

Individual clones recognizing MMP-9 were inoculated in 5 mL SD-CAA (-Trp, -Ura) cultures, grown to saturation, and induced. To determine antibody affinity, titration assays were conducted. These experiments followed the preparation of flow cytometry, using previously described techniques[46], with the following alterations: 15,000 cells per sample were incubated with agitation for 30 minutes (as opposed to the standard overnight given degradation effects observed with single clone binders M0076 and DX-2802) with anti-c-Myc antibody (1:500) and MMP-9 ranging in concentration from 1 μM to <1 nM. Flow analysis focused on the normalized median fluorescence intensity as a function of MMP-9 concentration to establish K_d values for all clones of interest.

2.4.8. Yeast Display Inhibitor Assay

To examine the binding versus inhibitive properties of isolated MMP-9 affinity reagents, a simple yeast display assay was developed. This assay follows the same initial preparation as a time course flow cytometry experiment, but switches to an FS-6 activation verification after primary labeling. By doing so, binding or inhibition of the activated MMP-9 by the scFv may be examined by the readout of a plate reader. As described in sections 2.2.3, the following protocol standards were established: 50x FS-6, 100 nM MMP-9, and 2e6 cells per sample (50 uL final resuspension volume), run for 15 minutes on the plate reader, following the settings for MMP-9 activation (excitation – 323 nm, emission – 398 nm).

Chapter 3: Multiplexed High-Throughput Screening with Yeast Display

3.1. Introduction

3.1.1. Overview

High-throughput screening (HTS) enables researchers to explore the near-infinite wasteland of sequence space made available through protein engineering and display library technologies. Standard HTS includes: automated high throughput sequencing (AHTS), immobilized affinity sorting (IAS), and flow cytometry and the related fluorescence-activated cell sorting (FACS). Each of these methods enables rapid isolation of affinity reagents, but only against single antigen targets (singleplex). More recently advanced methods – DNA-barcoding, *in vitro* compartmentalization, PACE, and others – enable the rapid generation and isolation of affinity reagents against multiple targets, but require considerable technical expertise. All methods also require specialized equipment and are costly in terms of time and materials[50].

Here, we present work on the start of a simple and robust, benchtop high-throughput screening system for the isolation of affinity reagents in multiplex using magnetic bead sorting. While as yet incomplete, we demonstrate the potential of the concept through model sorting and provide advances in the understanding of requirements to establish such a process, leaving the project poised for future development.

3.1.2. High-Throughput Screening

High-throughput screening enables rapid and selective enrichment and isolation of engineered proteins with the desired phenotype, enabling researchers to cover broader swaths of sequence space.

3.1.2.1. Standard Techniques

Widely used in the biotechnology, pharmaceutical, and institutional research industries, standard high-throughput screening methods include: automated high-throughput screening (AHTS), immobilized antigen sorting (IAS), and flow cytometry, described in Chapter 1, Section 1.1.3.

AHTS is widely used within the biotechnology and pharmaceutical industries, but at great expense and, often, with technical difficulties (Fig. 22A). A well-organized flow cytometer enables the rapid screening of up to 1e8 mutants per hour, and can be combined with the popular FACS to separate differentially fluorescent cells as a proxy for antigen binding (Fig. 22B). Finally, immobilized antigen sorting varies in type (bead, glass slide, etc.) but involves attachment of target antigens to a solid support and incubation with the target, washing off the unbound proteins, to enrich only for those which bind the target antigen. Among immobilized antigen sorting, magnetic bead based sorting and the more specialized magnetic activated cell sorting (MACS, Fig. 22C) are perhaps both the most simplistic and high throughput – utilizing antigens bound to magnetic beads and pulling the magnetic beads out of solution.

Each of these methods is effective, but costly, and often requires significant time, labor, and specialized equipment to be successful. In addition, each is

currently, limited to the isolation of a single target protein (singleplex), though automated high throughput screening can yield multiple results by performing the same operation in parallel.

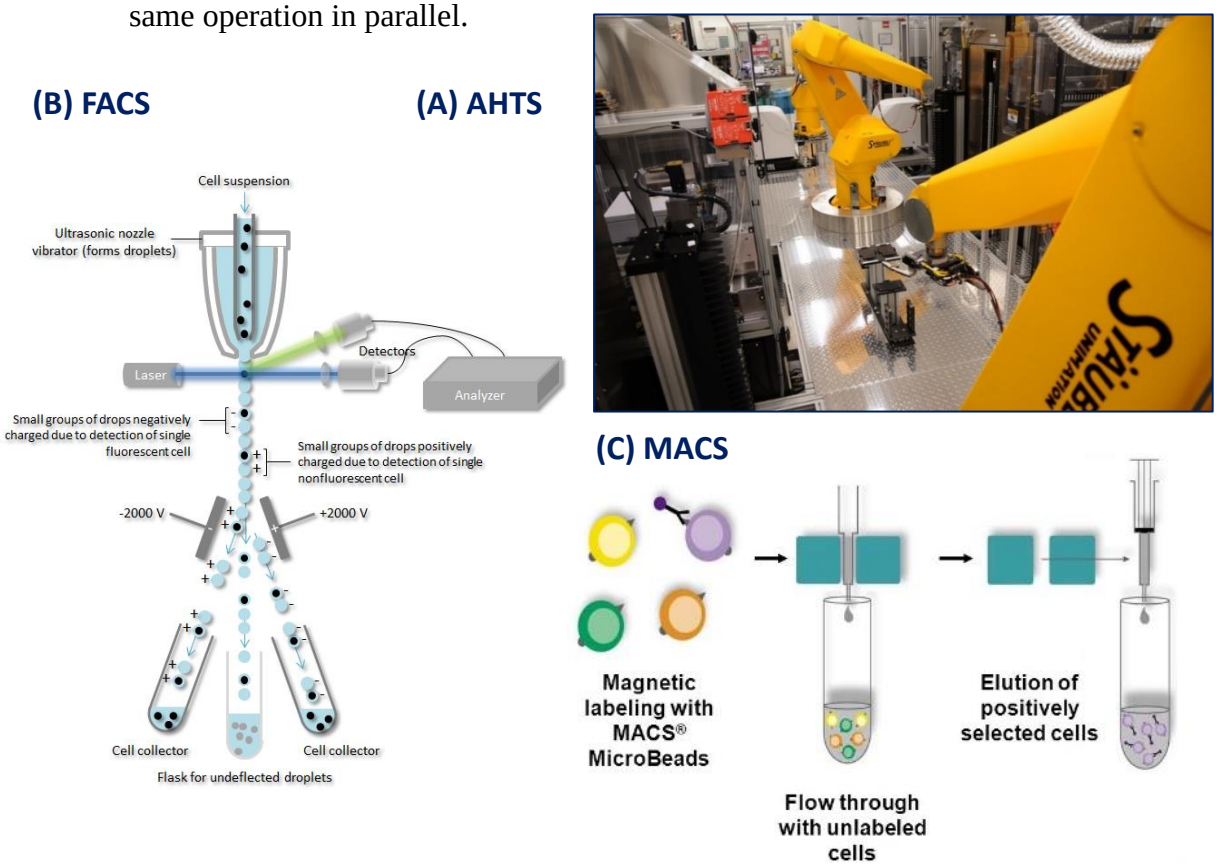

Figure 22. Industry standard high-throughput screening methods
(A) Automated High Throughput Screening, *Figure adapted from National Center for Advancing Translational Science*[83] **(B)** Fluorescence-Activated Cell Sorting, *Figure adapted from Sino Biological*[75] **(C)** Magnetic-Activated Cell Sorting, *Figure adapted from Medilab Korea*[84].

3.1.2.2. Recently Developed Methods

In recent years, new techniques have joined the ranks of high-throughput screening methods, some of which enable multiplexed screening. The more utilized of these methods include: DNA-barcoded libraries, *in vitro* compartmentalization, and phage-assisted continuous directed evolution (PACE)[50].

DNA-barcoded libraries enable library-against-library screens by preparing proteins that are barcoded with a DNA sequence using *in vitro* translation and ribosome display, or individually via enzymatic conjugation (Fig. 23A). These barcoded and displayed proteins are then collectively assayed in aqueous solution, and analyzed by immobilization in a thin polyacrylamide layer, in which the individual proteins are identified and quantified by amplification of the DNA barcode. This technique allows precise quantification of protein interactions, measured on the basis of statistics of colocalized polonies arising from barcoding DNAs of interacting proteins, enabling simultaneous assessment of affinity and specificity (Fig. 23B)[76].

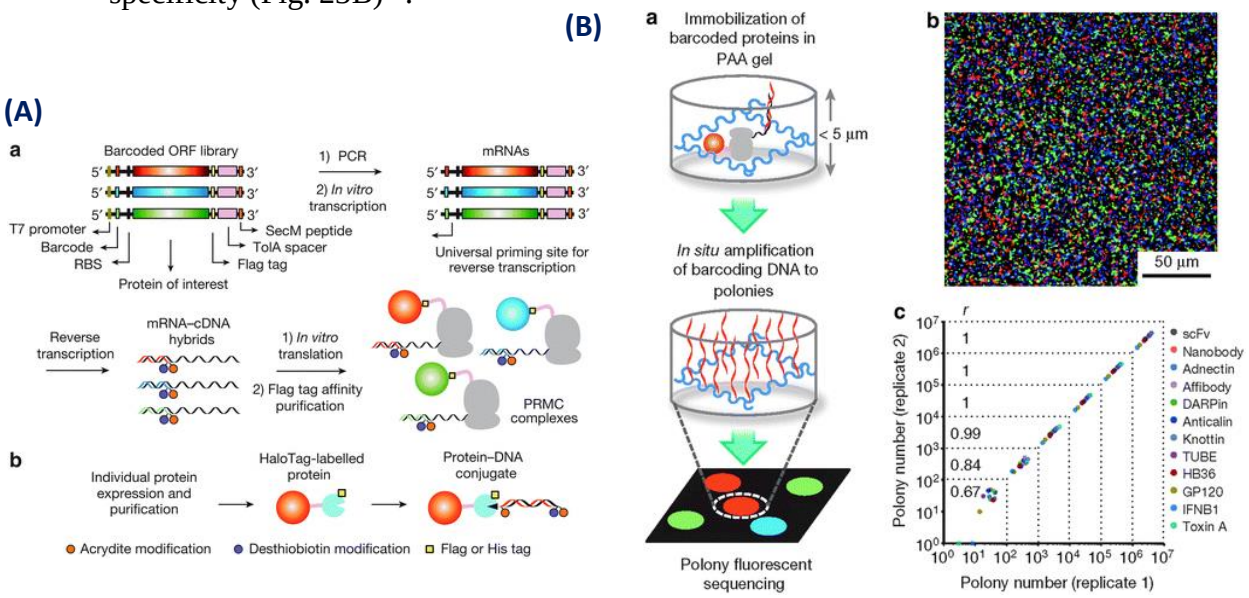

Figure 23. DNA-barcoded libraries

(A) Representation of DNA-barcoding methods (a) collective barcoding via ribosome display, and (b) individual barcoding via HaloTag-mediated conjugation. **(B)** Amplification and quantification of DNA-barcoded libraries (a) schematic of immobilization and amplification, (b) merged polonies with labeled oligonucleotides, (c) polony quantification. *Figures adapted from Multiplex single-molecule interaction profiling of DNA-barcoded proteins, Gu et al, 2014*[76].

Various forms of *in vitro* compartmentalization (IVC) employ similar formats in which individual reactions of genes, gene products, and fluorogenic substrates are isolated and completed in droplets, often, water-oil emulsions. IVC enables proteins evolution in two formats: (1) emulsion of single cells expressing a library member, or (2) individual DNA molecules together with *in vitro* transcription-translation machinery. To screen these mixtures using FACS, a secondary emulsion (water-oil-water) is necessary to meet the requirements of particles in aqueous mixture. Through the flexibility of fluorogenic substrates within the droplets, the phenotypes and enzymes that can be screened increase[77].

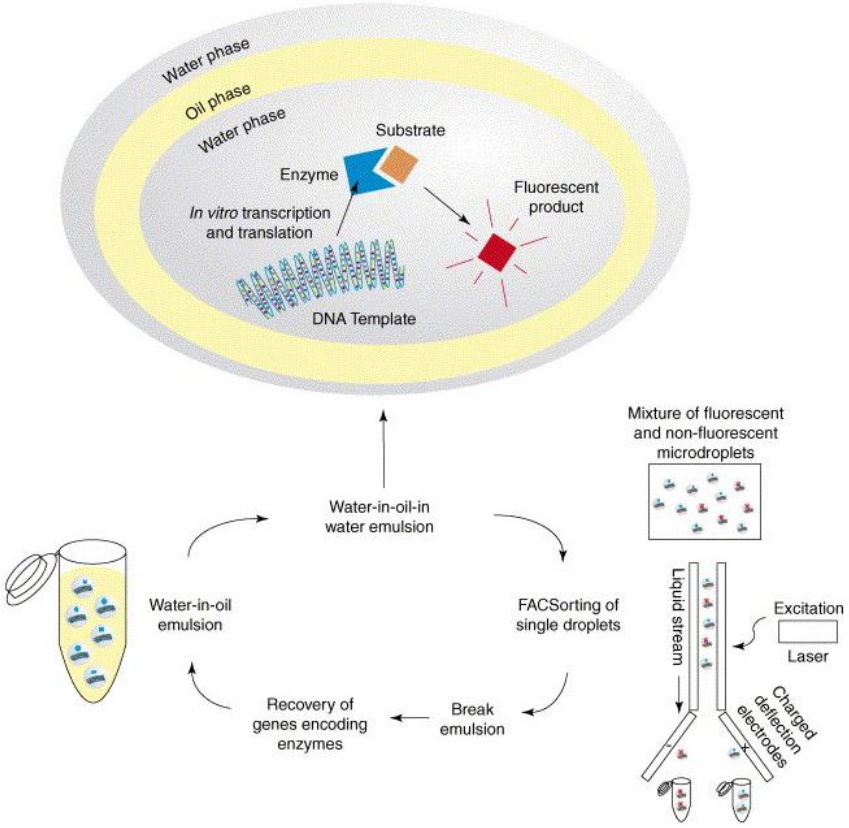

Figure 24. In vitro Compartmentalization

Representation of emulsion-based IVC using *in vitro* transcription/translation machinery for individual reactions for continuous FACS and evolution of enzymes. *Figure adapted from "Novel proteins in emulsions using in vitro compartmentalization", Rothe et al, 2006.*

Phage-assisted continuous evolution (PACE) makes use of the M13 bacteriophage infection cycle by placing an evolving gene into the M13 genome in place of an essential gene; often, gene III (gIII) which triggers production of pIII. The evolving gene then controls expression of gIII from an accessory plasmid; if a functional library protein is produced, then pIII is encoded. Only phage assembled with pIII are infectious, and so through repeated rounds of PACE the library will be enriched for members that better enable bacterial infection and replication. The continuous nature of this process enables several hundred "rounds" of selection, mutation, and replication to take place per week without manual intervention.

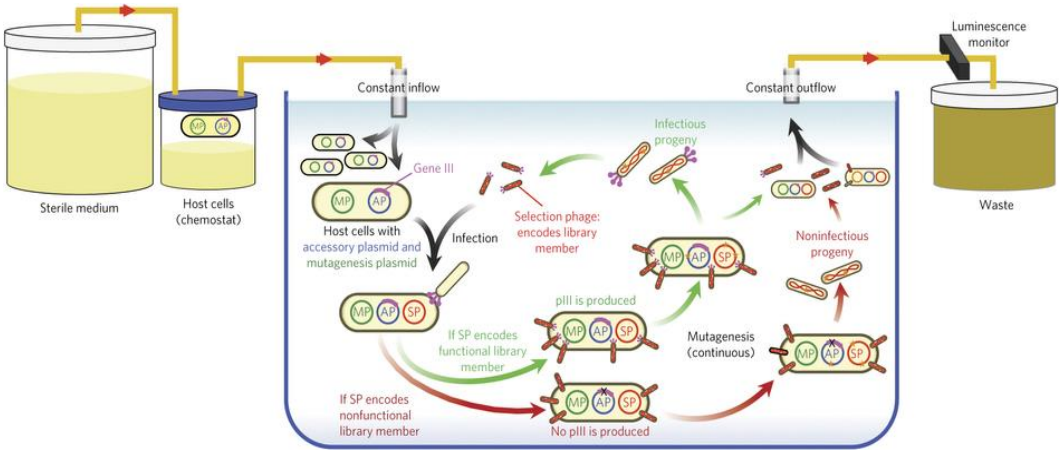

Figure 25. Phage-assisted continuous evolution (PACE)
Representation of PACE. Host *E.coli* flow continuously into a fixed-volume vessel (lagoon) containing filamentous phage that encode the library of evolving proteins. The lagoon is continuously drained after passing through an in-line luminescence monitor to measure expression of gIII. Dilution occurs faster than cell division, but slower than phage replication. Phage encoding less active library members produce fewer infectious progeny and so are lost by dilution. *Figure adapted from "Negative selection and stringency modulation in phage-assisted continuous evolution," Carlson et al, 2014.*

While these and other high-throughput screening advances are effective and capable of multiplex, they require a high level of technical expertise, and each requires at least one form of specialized equipment, limiting their accessability.

3.1.3. Research Objectives

The overarching goal of this thesis project is the establishment of a benchtop process for multiplex magnetic bead sorting to advance a simple and robust, high-throughput screening platform. Ideally this method will enable the simultaneous screening of display libraries against various proteins types, including proteolytic enzymes, for massive parallel processing and significantly increased enrichment efficiency, while also enabling enrichment of cross-reactive affinity binders.

To examine this increased efficiency, Figure 26 presents a simple calculation to compare the isolation of 10 antigens using singleplex and multiplex magnetic bead sorting. In Fig. 25A, we see the standard schedule for multiplex bead sorting, taking into account the initial library inoculation and induction, before beginning the standard two day rotation of sort + rescue growth on one day (Fig. 26A, Day 3), and magnetic bead rescue and induction on the second (Fig. 26A, Day 4), before performing a new sort on the following day (Fig. 26A, Day 5). Figure 26B then makes the assumption that within 4 rounds of sorting, a sufficient population of binders will have been enriched – as was seen with the isolation of Donkey IgG binders in Section 2.2.4.3. With this, it can be estimated that isolation of binders will be completed within 2 weeks through multiplex, but will require greater than 12 weeks through singleplex, resulting in a greater than 6 fold increase in efficiency.

(A)

Day 1 Day 2 Day 3 Day 4 Day 5

Inoculate → Induce → Sort + Rescue Growth → Induce → Sort → Repeat

(B)

Singleplex

$$\begin{pmatrix} 1\ Antigen \\ Sort \end{pmatrix} = 2\ Days + \frac{2\ Days}{Round} * \frac{4\ Rounds}{Sort} * 10\ Antigens = 82\ Days$$

$$= \sim \mathbf{12\ Weeks}$$

~6x faster

Multiplex

$$\begin{pmatrix} 10\ Antigens \\ Sort \end{pmatrix} = 2\ Days + \frac{2\ Days}{Round} * \left(\frac{4\ Mx.Rounds}{Sort} + \frac{2\ Indiv.Rounds}{Sort} \right) = 14\ Days$$

$$= \sim \mathbf{2\ Weeks}$$

Figure 26. Singleplex v. Multiplex Magnetic Bead Sorting Efficiency
(A) Standard magnetic bead sorting schedule, **(B)** Comparative singleplex and multiplex magnetic bead sorting time calculations

3.2. Results and Discussion

To ensure a robust process, various bead types and quantities were examined starting with model sorts of known antigen concentrations before moving to screening with libraries to examine and compare singleplex and multiplex enrichment efficiency.

3.2.1. Model Sorts

Model magnetic bead sorts focused on isolation of two standard proteins of interest: lysozyme and human fibroblast activation protein (hFAP). Initial experiments focused on customary target displaying: dilution displaying cell concentration ratios of 1:100; 1:1,000; and 1:10,000. Sorts with more ambitious ratios of 1:1,000,000 were then performed in singleplex and multiplex, approaching a mimic of potential library conditions (if a yeast display library contains 1e9 cells, it will optimally also contain 100 clones for the target of interest, thus equating to a target displaying: diluting displaying concentration of 1:1e7). All sorts examined two magnetic bead ratios of 10 µL and 50 µL to compare enrichment efficiency. Additionally, varied bead ratios (1:1, 1:10) were tested with the model sorts to examine the potential impact of having target antigen-coated beads mixed with non-target antigen-coated beads during and enrichment. By this, if 10 uL of magnetic beads were added, and diluted in a 1:10, there would be 1 uL of magnetic beads coated in the target antigen, and 9 uL of magnetic beads untouched.

Model sorts proceeded as expected for validation of technique and binding clones, but with no discernible difference in enrichment against 10 µL or 50 µL of

magnetic beads, and so both bead volumes were carried through to the initial multiplex magnetic bead library sorts.

3.2.1.1. Singleplex Model Sorts – 1:100; 1:1,000; 1:10,000

The initial model bead sorts resulted in the fold enrichments of 80+, 200+, and 1,000+, as expected when performing model bead sorts against the respective 1:100; 1:1,000; and 1:10,000 model cell ratios (Figure 27, A & B). Encouragingly, when performing magnetic bead sorts with the varied bead ratios of 1:1 and 1:10, the enrichment observed was equal to or greater than the dilution ratio of the magnetic beads (Figure 28). This suggests that multiplex magnetic bead sorting may provide the high efficiency screening desired. Additionally, the use of 50 µL of diluted magnetic beads, demonstrated a notable increase in overall enrichment to the target, suggesting that a larger bead volume still warranted further exploration for enrichment efficiency.

3.2.1.2. Multiplex Model Sorts – 1:100 and 1:10,000

Likewise, when performing multiplex sorts against both hFAP and lysozyme displaying binders diluted within a population of EGFR-displaying binders, fold enrichment remained greater than or near optimal (Figure 29). No clear and significant difference was noted between 10 µL and 50 µL of magnetic beads, and so both bead volumes were carried forward.

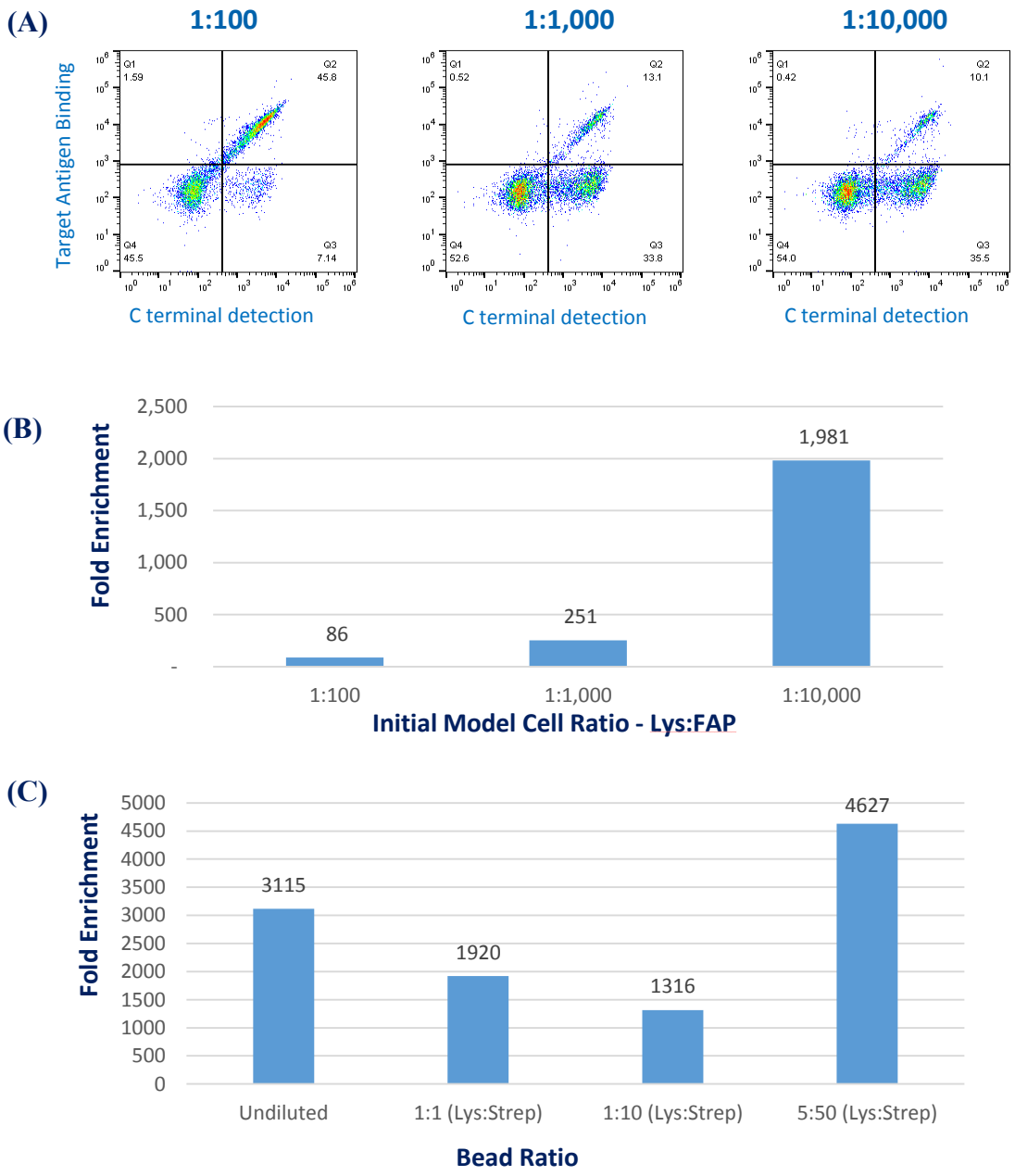

Figure 27. Initial Model Magnetic Bead Sorts

Flow cytometry data associated with singleplex magnetic bead sorting for lysozyme displaying binders and diluting with FAP displaying binders, average of triplicate sorts. **(A)** Cell ratios of target:diluent – 1:100; 1:1,000; and 1:10,000, **(B)** Corresponding fold enrichment Singleplex – varied cell ratios, **(C)** Fold Enrichment: Cell ratio target:diluent – 1:10,000, magnetic bead ratios (lysozyme-coated:streptavidin-coated) – Undiluted, 1:1, 1:10, 5:50.

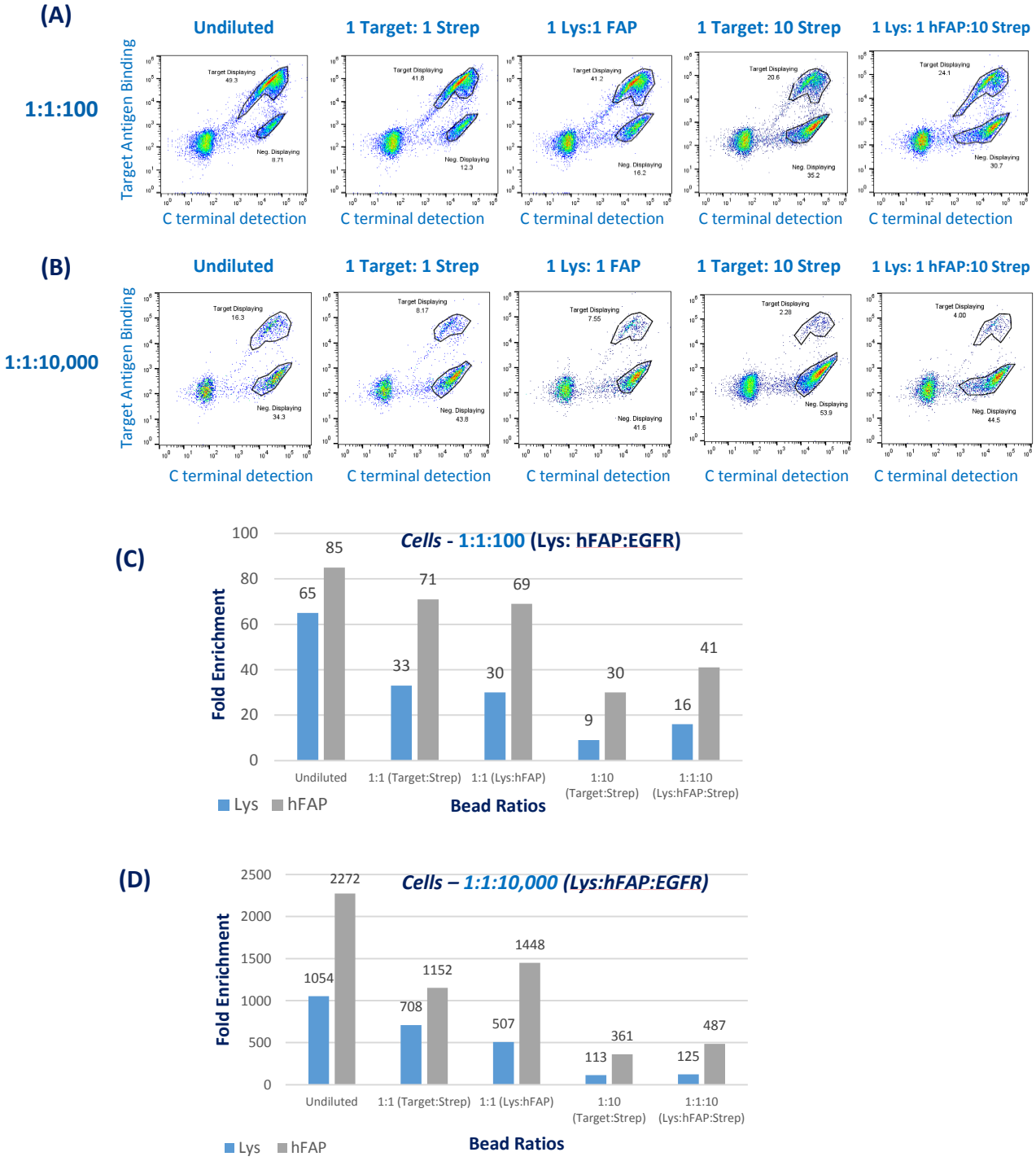

Figure 28. Initial Multiplex Model Magnetic Bead Sorts

Flow cytometry data for associated with multiplex magnetic bead sorting for hFAP (shown) and lysozyme (multiplex targets) displaying binders, diluting with EGFR displaying binders. Magnetic bead ratios explored: Undiluted, Target:Streptavidin, hFAP:Lys, (1 Target):(10 Streptavidin), (1 hFAP):(1 Lys):(10 Streptavidin). **(A)** Cell ratios of target:diluent – 1:1:100; and **(B)** 1:1:10,000. **(C, D)** Corresponding flow enrichment, (C) Cell Ratio –1:1:100, (D) Cell ratio – 1:1:10,000.

3.2.1.3. Library Mimic Multiplex Model Sorts – 1:1,000,000

Magnetic bead sorts against cell ratios approaching a mimic of library conditions were performed in singleplex and multiplex conditions (if a yeast display library contains 1e9 cells, it will optimally also contain 100 clones for the target of interest, thus equating to a target displaying: diluting displaying concentration of 1:1e7). The resulting fold enrichments demonstrated that simple, multiplex sorting is able to generate enrichment at levels equal to or greater than the bead ratio dilution (1:1 or 1:10) resulting from multiplexing. Additionally, fold enrichments of greater than 100,000 within one round, and over 900,000 within two rounds, were demonstrated. This suggests that the maximum accepted fold enrichment value of 30,000[52] may be improved.

(A) ***Initial Cell Ratio*** **– Lys:hFAP:EGFR** – 1:1:1,000,000

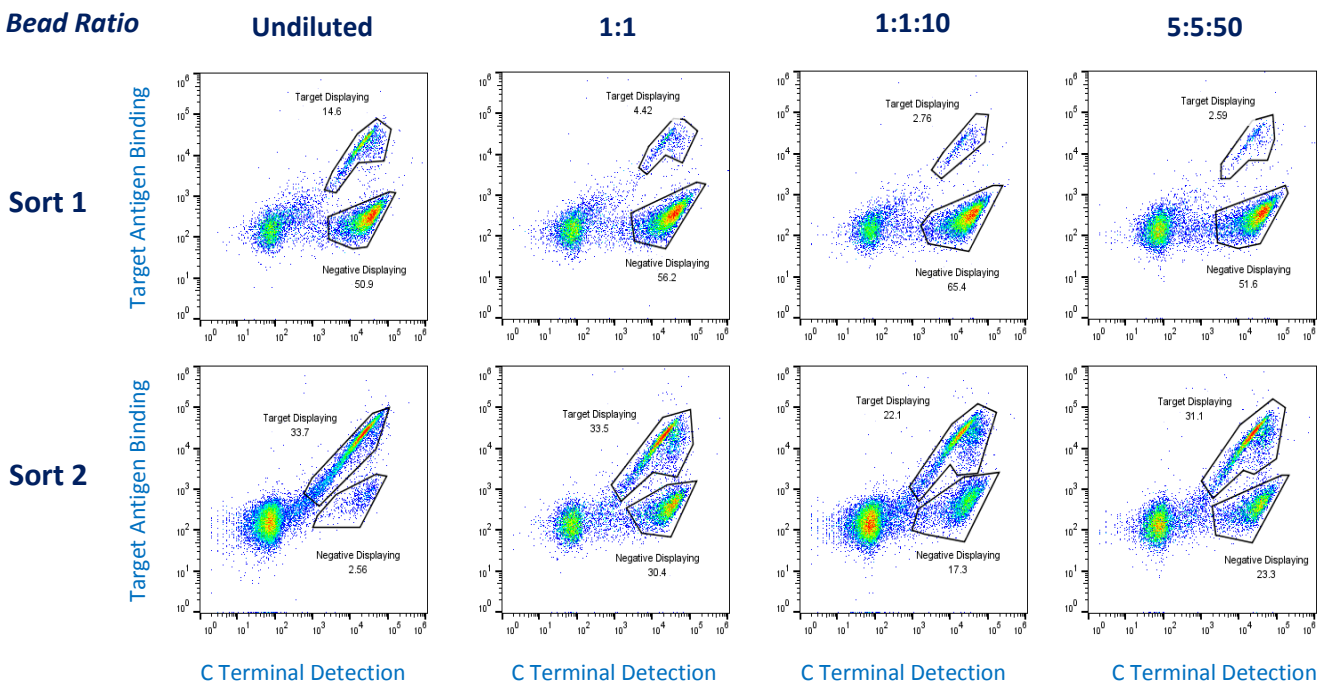

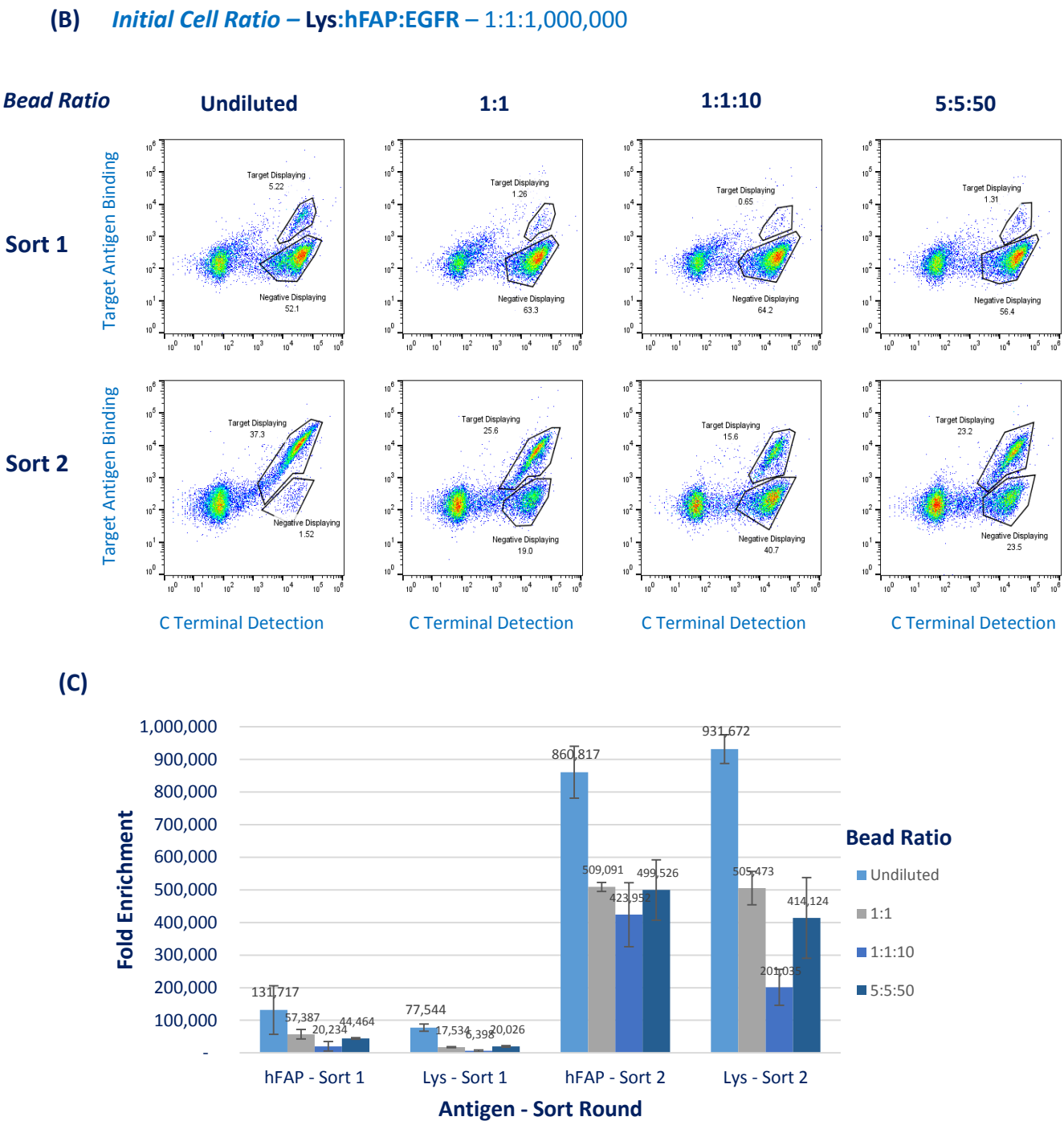

Figure 29. Library Mimic Multiplex Model Magnetic Bead Sorts

Flow cytometry data associated with multiplex magnetic bead sorting for **(A)** hFAP and **(B)** lysozyme (targets) displaying binders, diluting with EGFR displaying binders. Bead ratios: Undiluted, (1 hFAP):(1 Lys), (1 hFAP):(1 Lys):(10 Streptavidin), and (5 hFAP):(5 Lys):(50 Streptavidin), with **(C)** Corresponding fold enrichment.

3.2.2. Singleplex

Once multiplexing was confirmed with library-mimicking model sorts (1:1,000,000), singleplex sorts were performed with Bovine, Goat, and Rabbit IgGs against the Sidhu Library to establish baselines of enrichment and clonal isolation for comparison with future multiplexing. When analyzing library sort enrichments, percent antigen binding is utilized instead of fold enrichment, as the number of binders within the library is unknown and so the enrichment ratios cannot be employed.

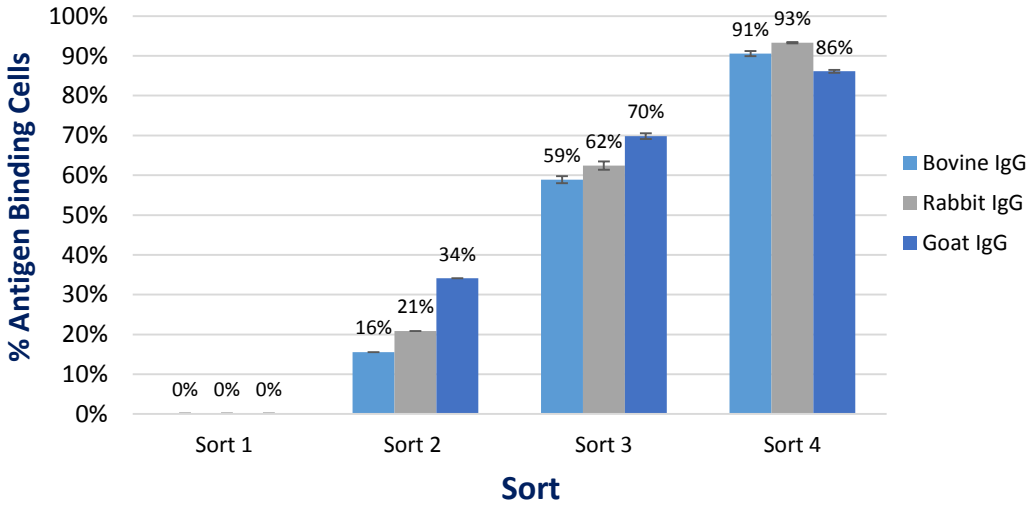

Figure 30. Sidhu Library – Singleplex IgG Magnetic Bead Sorts
Percent antigen binding results of four rounds of magnetic beard sorting against single IgG targets with the Sidhu Library.

3.2.3. Multiplex – Sidhu Library

With baselines for enrichment and clonal isolation established for comparison, multiplexing was then performed against various combinations of 14 antigens of interest: Bovine, Goat, and Rabbit IgGs, Chymotrypsin, human Hemoglobin (hH), Lysozyme, RNase A, Trypsin, human and murine DPP-IV,

human and murine FAP, and human and murine MMP-9. As described in the Experimental Methods, DPP-IV and FAP were enzymatically biotinylated, all other proteins were chemically biotinylated.

These sorts examined more standard antigen targets for proof of concept (IgGS hH, Lysozyme, RNase A); to examine the potential of isolating cross-reactive binders when multiplexing against similar proteins (IgGs); against proteolytic enzymes (chymotrypsin, trypsin) to examine the possibility of multiplexing proteins with proteolytic enzymes, despite the exploration of libraries not specifically designed for enzymatic binder isolation; and against more physiologically interesting enzyme targets (DPP-IV, FAP, and MMP-9).

3.2.3.1. Initial Multiplex Sorts

Results of the initial multiplex magnetic bead sorts immediately highlighted the challenge multiplexing introduces: the enrichment of cross-reactive binders against proteins and protein complexes other than the individual targets. Namely, the enrichment of binders against the excess biotin found of the surface of some proteins as a result of chemical biotinylation.

The first multiplex magnetic bead sorts focused on ten antigen targets: bovine, goat, and rabbit IgGs, chymotrypsin, human hemoglobin, human and murine FAP, lysozyme, human and murine MMP-9 RNase A, and trypsin. With each round of sorting, the isoform of FAP and MMP-9 would alternate so that cross-reactive binders would be enriched. Both 10 µL and 50 µL of beads were used for

enrichments, and flow cytometry was performed after each round of sorting against each antigen from within the enriched mixture.

Within four rounds of sorting (Figure 31), and with both volumes of beads, percent antigen binding for the three IgGs, human hemoglobin, lysozyme, MMP-9 and RNase A were between 15% and 60%. Percent antigen binding against chymotrypsin and trypsin demonstrated some small measure of success between ~2% and 7%, with clear indications of cleavage by the active enzymes, and FAP showed mild enrichment between ~2% and 4% antigen binding. That the sum of percent antigen binding was well over 100% indicated that cross-reactive or nonspecifically sticky enrichment was occurring. Performing individual sorts against the multiplex enriched populations from this fourth round and then running flow cytometry experiments against the singly isolated populations with different target proteins (example: isolated rabbit IgG, flow cytometry labeling with murine MMP-9) demonstrated that for all but one protein (FAP), the enriched populations were substantially binding to each of the other targets. This suggested that enrichment for cross-reactive binders was occurring. That FAP was not demonstrating this cross-reactive binding profile, in turn, suggested that the deciding factor was the biotinylation process (chemical for all antigens except FAP and DPPIV, which were enzymatic).

One distinct possibility revolved around the additional biotin molecules present on the other protein targets as a result of chemical biotinylation, and that enrichment for biotin or biotin complexes as opposed to pure target antigens was occurring. It was also possible that the secondary fluorophore being employed for

flow cytometry experiments – Streptavidin AF488 – was leading to complexing events with the biotinylated antigens, and so skewing the flow results. Further, no significant enhancement of enrichment was noted by the use of 50 µL of magnetic beads as opposed to 10 µL, and so experiments moving forward employed only the standard volume of 10 µL.

3.2.3.2. Biotinylation Experiments

To test the biotin-binder enrichment hypothesis, further sorts were performed in which the library was first depleted of streptavidin and biotin binders. Free biotin was then added to the cell populations to preemptively attach to any biotin-binders that may have avoided depletion, before positive multiplex sorts against target proteins were performed. Once enrichments reached ~5%-10% per target proteins (nearing 100% total percent antigen binding), individual sorts were performed. These individually enriched proteins were then examined using flow cytometry competition experiments (described in Section 3.5.2), to test for non-specific binding (Figure 32, "Standard").

For competition experiments (Figure 32, "Competition") comparing the biotinylated antigen and stock antigens, during primary labeling the cells were first incubated with stock antigen for 15 minutes (400 nM), then the biotinylated antigen was added (20 nM) for another 30 minutes. If the enrichment was happening against only the target of interest, and not the biotin-antigen complex, then the resulting event plots would be ~1/20 of the normal outcome as the stock antigen would have bound the majority of potential binding clone sites without being outcompeted.

Examining the results in Figure 32, we see from the competition experiments that – despite the depletion sorts against biotin – the binders isolated against chemically biotinylated antigen targets did not preferentially bind to the vast excess of non-biotinylated antigen used as the primary label, but bound instead to the chemically biotinylated proteins. The one exception to this remained the enzymatically biotinylated FAP, which showed a clear and significant decrease in binding when non-biotinylated antigen was added, dropping from over 30% antigen binding, to less than 2% antigen binding. This suggests that the cross-reactive or nonspecific isolation being observed may result from the biotinylation method employed.

To test the secondary fluorophore labeling hypothesis, fluorophores (secondary reagents) specific to FAP (based on binding to their murine Fc region) and to MMP-9 were employed for those antigens within the multiplexed mixture. No change was observed for multiplex enriched MMP-9, suggesting that secondary fluorophore complexing is not the issue at hand.

(A) 10 µL Beads

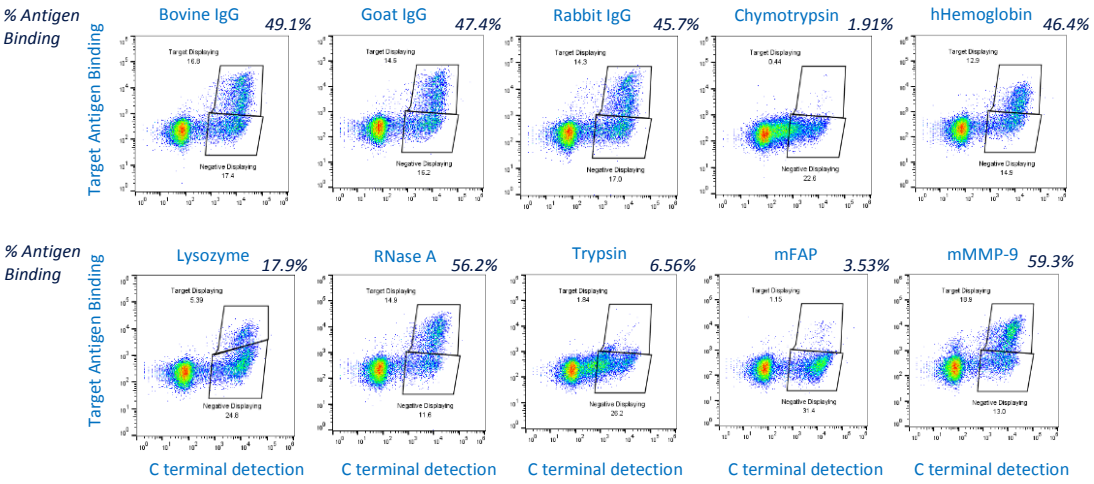

(B) 50 µL Beads

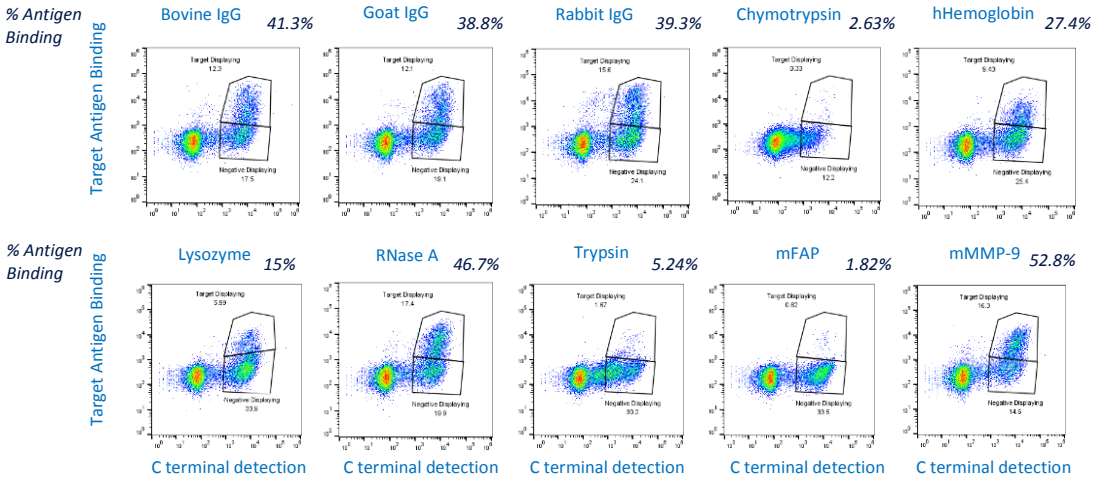

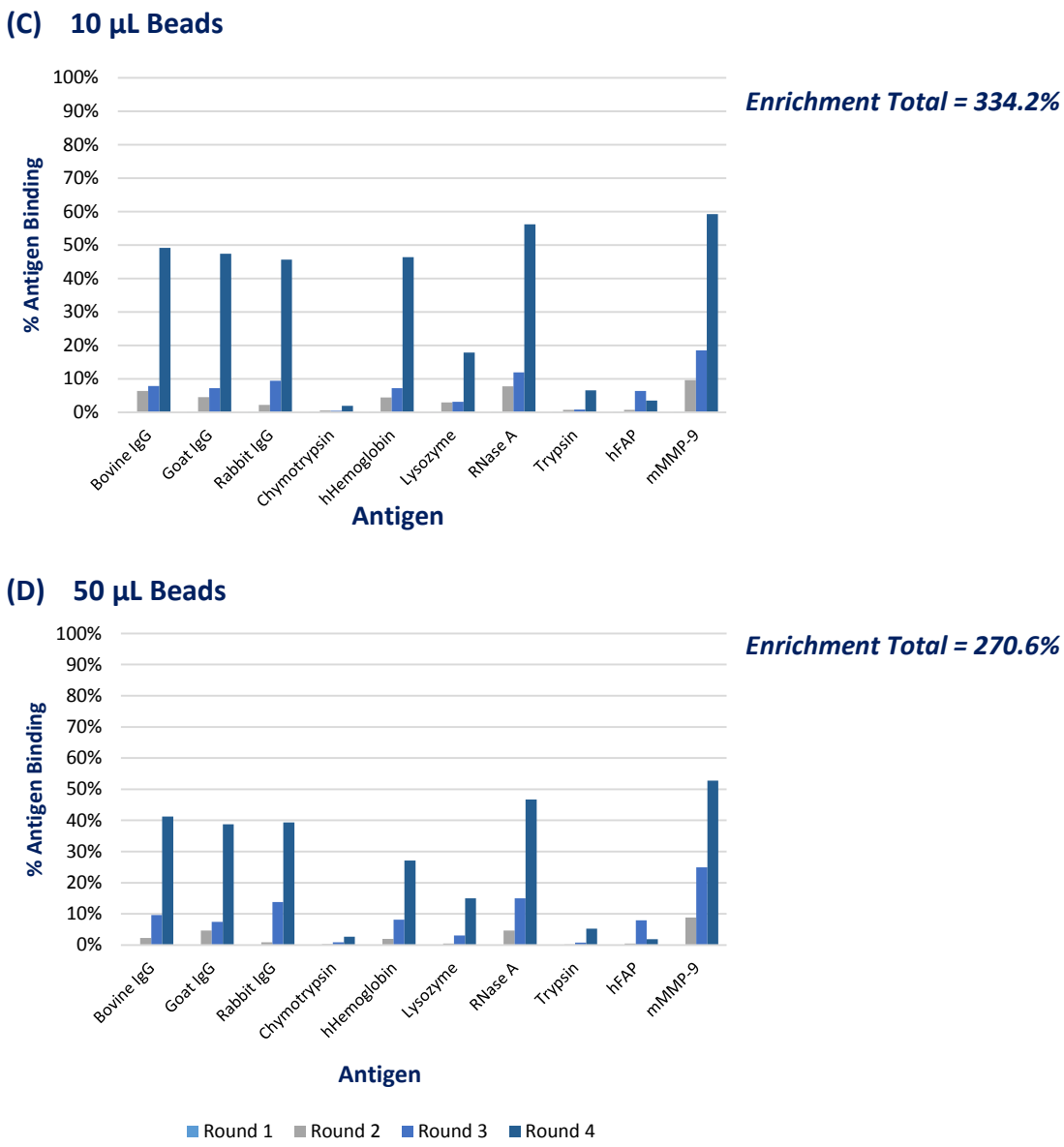

Figure 31. Multiplex magnetic bead sorting – Initial Sorts

(A & B) Include flow cytometry data with associated percent antigen binding, run for each of the 10 protein targets enriched against, for both 10 and 50 µL of magnetic beads. **(C & D)** Corresponding percent antigen binding for each of the 10 protein targets, with total enrichments for each sorted population.

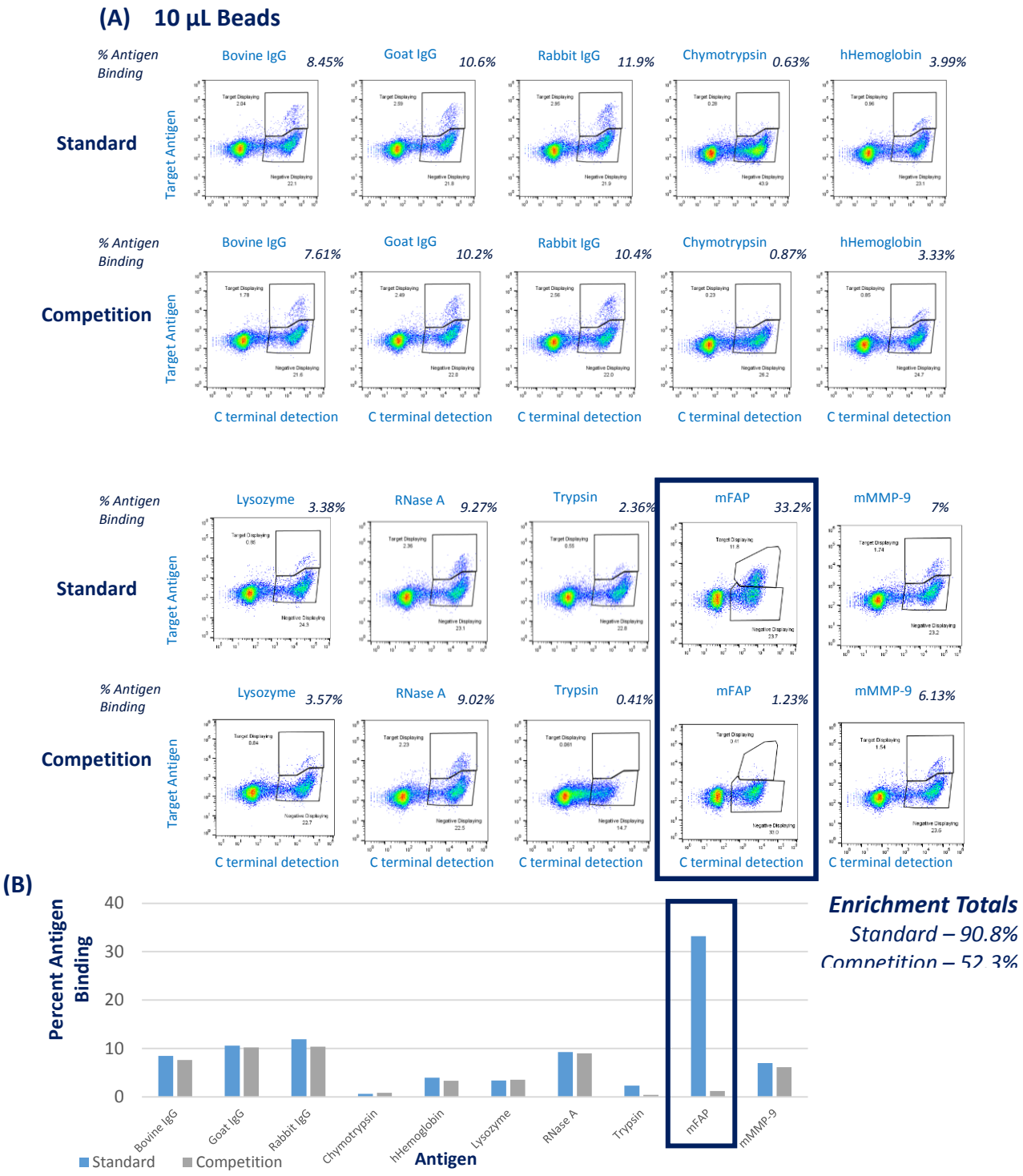

Figure 32. Multiplex magnetic bead sorting – Depletion Sorts and Competition Experiments

(A & B) Include flow cytometry data with associated percent antigen binding, run for each of the 10 protein targets enriched against, for both 10 and 50 µL of magnetic beads. **(C & D)** Corresponding percent antigen binding for each of the 10 protein targets, with total enrichments for each sorted population.

3.3. Conclusions

Multiplexed magnetic bead sorting, though simple in concept, has proven to be a challenging approach to develop. The enrichment of cross-reactive or nonspecifically sticky binders despite targeted depletions against likely culprits, and the addition of free biotin to block potential nonspecific binding sites suggest that more complex molecular interactions may be occurring between target antigens and magnetic beads during sorting. However, the lack of cross-reactive FAP binders observed compared to other protein targets suggests that the chemical biotinylation of these antigens may be the cause. Utilized for its simplicity and ability to biotinylate even unknown proteins, chemical biotinylation does not affect single sites, but any exposed amine. Alternative processes, though more limited, may overcome the cross-reactive enrichment problem. Enzymatic biotinylations, in particular, could potentially enable multiplex magnetic bead sorting to succeed.

3.4. Experimental Methods

All materials and methods outlined in the following sections of Chapter 2, Section 2.6: Experimental Methods, pertain and apply in Chapter 3: Section 2.4.1 – Cell Culture, Section 2.4.3 – Magnetic Bead Sorting, Section 2.4.4 – Flow Cytometry, and Section 2.4.7 – Clonal Isolation and Characterization.

3.4.1. Protein Preparation

3.4.1.1. Construct Preparation

MMP-9, DPP-IV, and FAP human and murine isoforms were expressed through transfection of the aforementioned HEK293-F cells. Human and murine isoforms of FAP and DPP-IV were produced using secretion vectors gWiz-Fc-hFAP-BirA and gWiz-Fc-mFAP-BirA, and gWiz-Fc-hDPPIV-BirA and gWiz-Fc-mDDPIV-BirA, respectively; constructed using previously described methods. These vectors incorporate a murine Fc region upstream of the protein of interest to aid in purification, and a BirA sequence for enzymatic biotinylation downstream of the protein of interest. Human and murine MMP-9 pCMV-ORF-His expression constructs were purchased from Sino Biological[74,75]. Constructs were sequenced (Eurofins) to ensure correct assembly, and maxiprepped from transformed DH5αZ1 *E.coli*, grown with kanamycin, for transfection into HEK-293F cells as described in section 1.2.2.1.4.

3.4.1.2. Protein Purification

6-8 days after transfection, the culture was harvested, cells filtered for supernatant-containing target protein, and supernatant pH-adjusted with 10x phosphate-buffered saline (PBS). Protein A resin (Genscript) was used to purify the

Fc fusion proteins DPP-IV and FAP, while Ni-TNA resin (Genscript) was used to purify MMP-9, following recommendations of the manufacturer. Concentrations of the eluted proteins were measured, protein gels run to ensure purity, and aliquots of 0.5 mg/mL were prepared in 50% glycerol (vol/vol) and flash frozen using liquid nitrogen for freezing prior to storage at -80°C. Enzymatic activity of the proteins was also confirmed, using the fluorogenic substrate FS-6 (Sigma) for MMP-9, and fluorogenic substrate Ala-Pro-7-amino-3-trifluoromethylcoumarine (Calbiochem) for DPP-IV and FAP.

3.4.1.3. Chemical Biotinylations

To prepare chemically biotinylated proteins from frozen or fridge protein stocks, EZ-Link NHS-LC-Biotin (ThermoScientific) was used. Frozen stocks of enzymes chymostrypsin, MMP-9, and trypsin were rapidly thawed in room temperature water, and then buffer exchanged into 1x phosphate-buffered saline (PBS; pH 7.4) using Amicon Ultra-0.5 30 kD MWCO devices, for storage at 4°C for up to 2 weeks. All other proteins – Bovine, Donkey, Rabbit, and Swine IgG, human hemoglobin, lysozyme, and RNase A - were stored at 4°C indefinitely. Chemical biotinylations were then performed using EZ-Link NHS-LC-Biotin (Thermo Scientific) with targeted biotinylation levels of 1-2 biotins per protein, verified using the Pierce Biotin Quantitation Kit (Thermo Scientific), and stored at 4°C for one week (previously frozen enzymes) or indefinitely.

3.4.1.4. Enzymatic Biotinylations

Fc-DPP-IV and Fc-FAP fusion proteins were enzymatically biotinylated using biotin ligase (Avidity). Frozen stocks were rapidly thawed in water at room temperature, and then buffer exchanged into bicine buffer (50 mM, pH 8.3) using Amicon Ultra-0.5 30 kD MWCO devices, for storage at 4°C for up to 2 weeks. 2.5 µL of biotin ligase BirA and 5 µL of Biomix B (100 mM ATP, 100 mM MgOAc, 500 µM d-biotin; Avidity BirA Biotin Ligase Kit) were added to 100 uL FAP or DPP-IV (1 mg/mL). Enzymatic reactions proceeded for 3 days on a 4°C rotary wheel; every 24 hours, additional Biomix B was added. Upon completion of the reaction, the mixture was buffer exchanged into FAP buffer using the Amicon Ultra devices. Success of enzymatic biotinylation was checked using flow cytometry. 10 µL of streptavidin-coated magnetic beads were incubated with biotinylated protein for 2 hours, then washed 3 times with ice-cold, 1x PBSA (pH 7.4). Protein-bound beads were then incubated with secondary label Alexa-Fluor 647 goat anti-mouse antibodies for 15 minutes, washed twice, and run through the flow cytometer.

3.4.2. Magnetic Bead Sorting

All model and multiplexed magnetic bead sorts utilized Biotin Binder Dynabeads (Thermo Scientific).

3.4.2.1. Model Sorts

Model magnetic bead sorts utilized RJY100 cells displaying clones expressing binders to human fibroblast activation protein (hFAP), lysozyme (Lys), and epidermal growth factor receptor (EGFR). hFAP and Lys binding clones served as both target and diluting populations, while EGFR-binder displaying cells

were always the diluting population. To mimic library sorting conditions, 1e9 cells of the diluting population were grown and induced. Target populations of: 1e7, 1e6, 1e5, and 1e3 cells were then added to form the respective 1:1e2; 1:e3; 1:1e4; and 1:1e6 ratios (Table 1). To perform multiplex model sorts, the same number of cells from both target populations (FAP and Lys binding clones) were added. To ensure accurate cell counts, OD_{600} measurements were taken of all induced cultures prior to combining.

When performing model bead sorts, enrichment is calculated by what is known as Fold Enrichment as opposed to Percent Antigen Binding (Equation 1). Through Fold Enrichment, the observed enrichment is compared to the known, original cell ratio using the following equation:

$$Fold\ Enrichment = \frac{Q2}{Q2+Q3} * \frac{1}{Initial\ Cell\ Ratio} \quad (2.1)$$

$$\frac{Target\ Displaying\ Population}{Total\ Displaying\ Population} * \frac{Diluting\ Population}{Target\ Population} \quad (2.2)$$

As with percent antigen binding, fold enrichment is often displayed through bar graphs to more easily visualize enrichment levels between screening rounds.

Ratio	Target Cells		Diluting Cells
1:100	10,000,000	+	1,000,000,000
1:1,000	1,000,000	+	1,000,000,000
1:10,000	100,000	+	1,000,000,000
1:1,000,000	1,000	+	1,000,000,000

Figure 33. Model magnetic bead sorts
Combinations of target displaying and diluting displaying cells.

3.4.2.2. Singleplex Enrichments

When performing singleplex magnetic bead sorting with multiple antigens from the same library, depletion sorts in which binders against biotin, streptavidin, and TA99 would be performed prior to splitting the culture for target antigen sorting to ensure that all sorts were beginning from the same population, following methods described inSectio 2.4.3 – Magnetic bead Sorting). The Sidhu Library had been previously enriched for hFAP, lysozyme, and EGFR binding clones by Professor James Van Deventer and other researchers, and so Bovine, Goat, and Rabbit IgGs were employed to establish further baselines prior to multiplexing.

3.4.2.3. Multiplex Enrichments

Multiplex magnetic bead sorting required preparation of the various antigen-coated magnetic beads individually, and so the magnetic bead and individual biotinylated antigen would be incubated separated and washed prior recombining to create a homogenous mixture to utilize in bead sorting.

3.4.3. Flow Cytometry: Multiplex Enriched Populations

When performing flow cytometry with multiplex sorted populations, samples in the same number as the number of antigens sorted against were prepared against the individual antigens (10 antigens, 10 samples). Once individual sorts against originally multiplexed populations were performed, comparative flow cytometry was performed against all other antigens in the set to ensure that only the target antigen was enriched against (perform multiplex sorting against bovine, goat,

and rabbit IgG; perform individual sorts against the 3 IgGs; run a flow cytometry experiment in which the multiplex population further enriched against only Bovine IgG is tested with all 3 IgGs to ensure specific isolation against solely the Bovine IgG target, and not cross-reactivity or polyspecificity against all three targets).

Further, two forms of competition flow cytometry was performed with non-biotinylated antigen, and biotinylated antigen in an attempt to confirm that only the antigen of interest was being enriched against and not biotin or the biotin-antigen complex. For competition experiments against biotin, during the primary labeling, biotin was first incubated with the cell populations for 15 minutes (400 nM), then the individual antigen (20 nM) was added for another 30 minutes. If the enrichment was happening against only the target of interest, we should see comparative flow cytometry results as the biotin would not have been bound nor interfere. For competition experiments comparing the biotinylated antigen and stock antigens, during primary labeling the cells were first incubated with stock antigen for 15 minutes (400 nM), then the biotinylated antigen was added (20 nM) for another 30 minutes. If the enrichment was happening against only the target of interest, and not the biotin-antigen complex, then the resulting event plots would be 1/20 of the normal outcomes as the stock antigen would have bound the majority of potential binding clone sites without being outcompeted.

Chapter 4: Conclusions

Inhibitors of matrix metalloproteinases for use as tool compounds to better understand the tumor microenvironment, and as therapeutics to combat cancer development and progression, have been a goal of researchers for over four decades. High throughput screening likewise requires novel and accessible methods for improved affinity binder isolation efficiency. In this work, the preliminary development of methods for the selection of matrix metalloproteinase-9 binders as a means of isolating MMP inhibitors is described. Multiplex magnetic bead sorting is further examined, and promising results demonstrated for improved high throughput screening efficiency.

A novel MMP activation protocol was first established, requiring only trypsin and a salt solution for rapid completion on the lab bench. Previously isolated binders of MMP-9, M0076 and DX-2802, were cloned into the yeast display platform, and tested for their binding and inhibitive properties. As expected, both clones bound to human MMP-9, and DX-2802 bound specifically to the activated form of the protein. Contrary to expectations, neither clone bound murine MMP-9.

These single clones were then combined with the activation protocol to begin development of an assay to compare binding versus inhibition of isolated single clone binders displayed on the yeast cell surface. While incomplete, the results of preliminary experiments are promising, proving able to differentiate between the binding M0076 and partially inhibitive DX-2802. This assay thus potentially offers a way to rapidly test for binding versus inhibition of isolated single clones.

Cross-reactive MMP-9 binders to active human and murine isoforms were then isolated from both the CDR-H3 and Sidhu Libraries, neither of which was designed for enzymatic binder isolation. Magnetic bead sorting and FACS were both used, demonstrating two means of potential binder selection. Donkey IgG binders were also isolated from the CDR-H3 Library after 4 rounds of magnetic bead sorting. Isolation of these binders not only served to validate the limited diversity of the CDR-H3 Library, but provides substantiation for expanded design of mini-libraries which can enable noncanonical amino acid incorporation for protein-small molecule hybrid design (Discussed further in Section 4.1 – Future Directions).

We further present the challenge of, and a potential means forward for, multiplex magnetic bead sorting, to simultaneously isolate specific binders against a multitude of antigens from a single protein display library population, enhancing high throughput screening efficiency. Multiplex sorting is first proved successful with model cell ratios and diluted magnetic bead ratios, isolating for two antigen target binders simultaneously with cell ratios up to 1:1:1,000,000. With library sort experiments, 9 of 10 antigen binders enriched displayed non-specific binding, but success was achieved with the enzymatically biotinylated FAP, while other proteins sorted against where chemically biotinylated.

4.1.1. Future Directions

The results presented in this thesis establish an exciting starting point for further establishment of methods to rapidly isolate and characterize MMP binders

to serve as direct inhibitors, or provide the basis of protein-small molecule hybrid design. In ongoing experiments, sequencing and characterization of isolated cross-reactive single clones against human and murine MMP-9 will confirm this method of isolation, and provide unique clones to further develop the yeast display inhibition assay. Characterization of these clones and the Donkey IgG binders will also enable additional analysis and validation of the CDR-H3 Library, thus justifying the creation of mini-libraries. Mini-libraries will take advantage of the simplicity of the protein diversity of the CDR-H3 Library to provide supplementary, chemical diversity through the incorporation of noncanical amino acids. These libraries could therefore lead to the high throughput discovery of protein-small molecule hybrids for highly selective binding and inhibition of MMPs, as well as other targets.

Finally, initial success isolating binders against enzymatically biotinylated FAP amidst failed isolation of chemically biotinylated antigens provides a clear next step in the development of multiplex magnetic bead sorting: the use of alternate biotinylation methods for the incorporation of a single biotin per target protein. The initial success of the model sorts and library sorting with FAP suggests that, through the addition of only a single biotin to the protein target, it may be possible to overcome the nonspecific isolation otherwise observed.

References

(1) Groff, K.; Brown, J.; Clippinger, A. J. *Biotechnol. Adv.* **2015**, *33* (8), 1787–1798.

(2) *Nat. Methods* **2015**, *12* (5), 373–373.

(3) Bradbury, A.; Plückthun, A. *Nature* **2015**, *518* (7537), 27–29.

(4) Kierny, M. R.; Cunningham, T. D.; Kay, B. K. *Nano Rev.* **2012**, *3*.

(5) Donzeau, M.; Knappik, A. Humana Press, 2007; pp 15–31.

(6) Holliger, P.; Hudson, P. J. *Nat. Biotechnol.* **2005**, *23* (9), 1126–1136.

(7) Frenzel, A.; Kügler, J.; Wilke, S.; Schirrmann, T.; Hust, M. Humana Press, Totowa, NJ, 2014; pp 215–243.

(8) Bird, R. E.; Hardman, K. D.; Jacobson, J. W.; Johnson, S.; Kaufman, B. M.; Lee, S. M.; Lee, T.; Pope, S. H.; Riordan, G. S.; Whitlow, M. *Science* **1988**, *242* (4877), 423–426.

(9) Schwartz, R. S. *N. Engl. J. Med.* **2004**, *350* (11), 1079–1080.

(10) Dostalek, M.; Gardner, I.; Gurbaxani, B. M.; Rose, R. H.; Chetty, M. *Clin. Pharmacokinet.* **2013**, *52* (2), 83–124.

(11) Grillo-López, A. J.; Hedrick, E.; Rashford, M.; Benyunes, M. *Semin. Oncol.* **2002**, *29* (1 Suppl 2), 105–112.

(12) Carter, P. *Nat. Rev. Cancer* **2001**, *1* (2), 118–129.

(13) Buss, N. A.; Henderson, S. J.; McFarlane, M.; Shenton, J. M.; de Haan, L. *Curr. Opin. Pharmacol.* **2012**, *12* (5), 615–622.

(14) Reichert, J. M.; Dhimolea, E. *Drug Discov. Today* **2012**, *17* (17–18), 954–963.

(15) Green, M. C.; Murray, J. L.; Hortobagyi, G. N. *Cancer Treat. Rev.* **2000**, *26* (4), 269–286.

(16) Schrama, D.; Reisfeld, R. A.; Becker, J. C. *Nat. Rev. Drug Discov.* **2006**, *5* (2), 147–159.

(17) Reichert, J. M. *Nat. Biotechnol.* **2001**, *19* (9), 819–822.

(18) Lambert, J. M. *Br. J. Clin. Pharmacol.* **2013**, *76* (2), 248–262.

(19) Chari, R. V; Martell, B. A.; Gross, J. L.; Cook, S. B.; Shah, S. A.; Blättler, W. A.; McKenzie, S. J.; Goldmacher, V. S. *Cancer Res.* **1992**, *52* (1), 127–131.

(20) Dubowchik, G. M.; Walker, M. A. *Pharmacol. Ther.* **1999**, *83* (2), 67–123.

(21) Peters, C.; Brown, S. *Biosci. Rep.* **2015**, *35* (4).

(22) Leal, M.; Sapra, P.; Hurvitz, S. A.; Senter, P.; Wahl, A.; Schutten, M.; Shah, D. K.; Haddish-Berhane, N.; Kabbarah, O. *Ann. N. Y. Acad. Sci.* **2014**, *1321*

(1), 41–54.

(23) Mullard, A. *Nat. Rev. Drug Discov.* **2013**, *12* (5), 329–332.

(24) Van Deventer, J. A.; Le, D. N.; Zhao, J.; Kehoe, H. P.; Kelly, R. L. *Protein Eng. Des. Sel.* **2016**, *29* (11), 485–494.

(25) Smith, G. P. *Science* **1985**, *228* (4705), 1315–1317.

(26) Wernérus, H.; Ståhl, S. *Biotechnol. Appl. Biochem.* **2004**, *40* (3), 209.

(27) Daugherty, P. S. *Curr. Opin. Struct. Biol.* **2007**, *17* (4), 474–480.

(28) Gai, S. A.; Wittrup, K. D. *Curr. Opin. Struct. Biol.* **2007**, *17* (4), 467–473.

(29) Beerli, R. R.; Bauer, M.; Buser, R. B.; Gwerder, M.; Muntwiler, S.; Maurer, P.; Saudan, P.; Bachmann, M. F. *Proc. Natl. Acad. Sci. U. S. A.* **2008**, *105* (38), 14336–14341.

(30) Zahnd, C.; Amstutz, P.; Plückthun, A. *Nat. Methods* **2007**, *4* (3), 269–279.

(31) *Protein Engineering and Design - Library construction for protein engineering*; Park, S., Cochran, J., Eds.; CRC Press, Taylor and Francis Group: Boca Raton, FL, 2010.

(32) *Protein Engineering and Design - Cell Surface Display Systems for Protein Engineering*; Park, S., Cochran, J., Eds.; CRC Press, Taylor and Francis Group, LLC: Boca Raton, FL, 2010.

(33) Söderlind, E.; Strandberg, L.; Jirholt, P.; Kobayashi, N.; Alexeiva, V.; Åberg, A.-M.; Nilsson, A.; Jansson, B.; Ohlin, M.; Wingren, C.; Danielsson, L.; Carlsson, R.; Borrebaeck, C. A. K. *Nat. Biotechnol.* **2000**, *18* (8), 852–856.

(34) Harel Inbar, N.; Benhar, I. *Arch. Biochem. Biophys.* **2012**, *526* (2), 87–98.

(35) Geyer, C. R.; McCafferty, J.; Dübel, S.; Bradbury, A. R. M.; Sidhu, S. S. Humana Press, Totowa, NJ, 2012; pp 11–32.

(36) Lloyd, C.; Lowe, D.; Edwards, B.; Welsh, F.; Dilks, T.; Hardman, C.; Vaughan, T. **2009**, *22* (3), 159–168.

(37) Rader, C. Humana Press, Totowa, NJ, 2012; pp 53–79.

(38) Thie, H.; Voedisch, B.; Dübel, S.; Hust, M.; Schirrmann, T. Humana Press, 2009; pp 309–322.

(39) Prassler, J.; Thiel, S.; Pracht, C.; Polzer, A.; Peters, S.; Bauer, M.; Nörenberg, S.; Stark, Y.; Kölln, J.; Popp, A.; Urlinger, S.; Enzelberger, M. *J. Mol. Biol.* **2011**, *413* (1), 261–278.

(40) Feldhaus, M.; Siegel, R. In *Flow Cytometry Protocols*; Humana Press: New Jersey, 2004; pp 311–332.

(41) Boder, E. T.; Raeeszadeh-Sarmazdeh, M.; Price, J. V. *Arch. Biochem. Biophys.* **2012**, *526* (2), 99–106.

(42) Angelini, A.; Chen, T. F.; de Picciotto, S.; Yang, N. J.; Tzeng, A.; Santos,

M. S.; Van Deventer, J. A.; Traxlmayr, M. W.; Wittrup, K. D. Humana Press, New York, NY, 2015; pp 3–36.

(43) Chao, G.; Lau, W. L.; Hackel, B. J.; Sazinsky, S. L.; Lippow, S. M.; Wittrup, K. D. *Nat. Protoc.* **2006**, *1* (2), 755–768.

(44) Mahon, C. M.; Lambert, M. A.; Glanville, J.; Wade, J. M.; Fennell, B. J.; Krebs, M. R.; Armellino, D.; Yang, S.; Liu, X.; O'Sullivan, C. M.; Autin, B.; Oficjalska, K.; Bloom, L.; Paulsen, J.; Gill, D.; Damelin, M.; Cunningham, O.; Finlay, W. J. J. *J. Mol. Biol.* **2013**, *425* (10), 1712–1730.

(45) Woldring, D. R.; Holec, P. V.; Zhou, H.; Hackel, B. J.; Hamers, R.; McKinney, E. *PLoS One* **2015**, *10* (9), e0138956.

(46) Van Deventer, J. A.; Kelly, R. L.; Rajan, S.; Wittrup, K. D.; Sidhu, S. S. *Protein Eng. Des. Sel.* **2015**, *28* (10), 317–325.

(47) Fellouse, F. A.; Esaki, K.; Birtalan, S.; Raptis, D.; Cancasci, V. J.; Koide, A.; Jhurani, P.; Vasser, M.; Wiesmann, C.; Kossiakoff, A. A.; Koide, S.; Sidhu, S. S. *J. Mol. Biol.* **2007**, *373* (4), 924–940.

(48) Persson, H.; Ye, W.; Wernimont, A.; Adams, J. J.; Koide, A.; Koide, S.; Lam, R.; Sidhu, S. S. *J. Mol. Biol.* **2013**, *425* (4), 803–811.

(49) Eigenbrot, C.; Randal, M.; Presta, L.; Carter, P.; Kossiakoff, A. A. *J. Mol. Biol.* **1993**, *229* (4), 969–995.

(50) Packer, M. S.; Liu, D. R. *Nat. Publ. Gr.* **2015**, *16*.

(51) Nolan, J. P.; Sklar, L. A. *Nat. Biotechnol.* **1998**, *16* (7), 633–638.

(52) Ackerman, M.; Levary, D.; Tobon, G.; Hackel, B.; Orcutt, K. D.; Wittrup, K. D. *Biotechnol. Prog.* **2009**, *25* (3), 774–783.

(53) Flow cytometry introduction | Abcam http://www.abcam.com/protocols/introduction-to-flow-cytometry (accessed Jul 16, 2017).

(54) Cathcart, J.; Pulkoski-Gross, A.; Cao, J. *Genes Dis.* **2015**, *2* (1), 26–34.

(55) Pattabiraman, D. R.; Weinberg, R. A. *Nat. Rev. Drug Discov.* **2014**, *13* (7), 497–512.

(56) Vihinen, P.; Kähäri, V.-M. *Int. J. Cancer* **2002**, *99* (2), 157–166.

(57) Itoh, T.; Tanioka, M.; Yoshida, H.; Yoshioka, T.; Nishimoto, H.; Itohara, S. *Cancer Res.* **1998**, *58* (5), 1048–1051.

(58) Chambers, A. F.; Matrisian, L. M. *J. Natl. Cancer Inst.* **1997**, *89* (17), 1260–1270.

(59) Murphy, G.; Knäuper, V. *Matrix Biol.* **1997**, *15* (8–9), 511–518.

(60) MURPHY, G.; STANTON, H.; COWELL, S.; BUTLER, G.; KNÄUPER, V.; ATKINSON, S.; GAVRILOVIC, J. *APMIS* **1999**, *107* (1–6), 38–44.

(61) Decock, J.; Thirkettle, S.; Wagstaff, L.; Edwards, D. R. *J. Cell. Mol. Med.*

2011, *15* (6), 1254–1265.

(62) Egeblad, M.; Werb, Z. *Nat. Rev. Cancer* **2002**, *2* (3), 161–174.

(63) Klein, T.; Bischoff, R. *Amino Acids* **2011**, *41* (2), 271–290.

(64) Overall, C. M.; Kleifeld, O. *Nat. Rev. Cancer* **2006**, *6* (3), 227–239.

(65) Turk, B. *Nat. Rev. Drug Discov.* **2006**, *5* (9), 785–799.

(66) Zucker, S.; Cao, J. *Cancer Biol. Ther.* **2009**, *8* (24), 2371–2373.

(67) Nicholson, S.; Wood, C.; Devy, L. Use of mmp-9 and mmp-12 binding proteins for the treatment and prevention of systemic sclerosis. WO2010045388A2, 2010.

(68) Ogata, Y.; Itoh, Y.; Nagase, H. *J. Biol. Chem.* **1995**, *270* (31), 18506–18511.

(69) Duncan, M. E.; Richardson, J. P.; Murray, G. I.; Melvin, W. T.; Fothergill, J. E. *Eur. J. Biochem.* **1998**, *258* (1), 37–43.

(70) Rosário, H. S.; Waldo, S. W.; Becker, S. A.; Schmid-Schönbein, G. W. *Am. J. Pathol.* **2004**, *164* (5), 1707–1716.

(71) Uchima, Y.; Sawada, T.; Hirakawa, K. *JOP* **2007**, *8* (4 Suppl), 479–487.

(72) InterPro. Trypsin, Chymotrypsin and Cancer https://www.ebi.ac.uk/interpro/potm/2003_5/Page2.htm (accessed Aug 13, 2017).

(73) Van Deventer, J. A.; Wittrup, K. D. In *Methods in molecular biology (Clifton, N.J.)*; 2014; Vol. 1131, pp 151–181.

(74) Human MMP9/MMP-9/CLG4B Gene ORF cDNA clone expression plasmid, C-His tag | SinoBiological http://www.sinobiological.com/Human-MMP-9-Gene-cDNA-Clone-(full-length-ORF-Clone),-expression-ready,-C-His-tagged_p61895.html (accessed Jul 20, 2017).

(75) Mouse MMP9/MMP-9/CLG4B Gene ORF cDNA clone expression plasmid, C-His tag | SinoBiological http://www.sinobiological.com/MMP-9-cDNA-Clone-g-18700.html (accessed Jul 20, 2017).

(76) Gu, L.; Li, C.; Aach, J.; Hill, D. E.; Vidal, M.; Church, G. M. *Nature* **2014**, *515* (7528), 554–557.

(77) Rothe, A.; Surjadi, R. N.; Power, B. E. *Trends Biotechnol.* **2006**, *24* (12), 587–592.

(78) Protein engineering - Latest research and news | Nature https://www.nature.com/subjects/protein-engineering (accessed Jul 21, 2017).

(79) Global Market For Biologics To Reach Nearly $252 Billion In 2017 https://www.bccresearch.com/pressroom/bio/global-market-biologics-reach-nearly-$252-billion-2017 (accessed Jul 21, 2017).

(80) Niu, G.; Cai, W.; Chen, X. *Front. Biosci.* **2008**, *13*, 790–805.

(81) Kessenbrock, K.; Plaks, V.; Werb, Z. *Cell* **2010**, *141* (1), 52–67.

(82) Lafleur, M. A.; Handsley, M. M.; Edwards, D. R. **2017**, *5* (22).

(83) Tox21 Collaboration Generates an Innovative Platform for Testing Individual Differences in Chemical Sensitivity | National Center for Advancing Translational Sciences https://ncats.nih.gov/pubs/features/chem-tox (accessed Jul 21, 2017).

(84) Medilab Korea; Brett McCormick. *Magnetic Cell Separation with AutoMACS (Pro)*; 2016.